Available online at www.sciencedirect.com

SciVerse ScienceDirect

Geochimica et Cosmochimica Acta 112 (2013) 208–225

Geochimica et Cosmochimica Acta

www.elsevier.com/locate/gca

Element abundances, patterns, and mobility in Nakhlite Miller Range 03346 and implications for aqueous alteration

Julie D. Stopar [a,*], G. Jeffrey Taylor [b], Michael A. Velbel [c], Marc D. Norman [d], Edward P. Vicenzi [e], Lydia J. Hallis [b]

[a] School of Earth and Space Exploration, Arizona State University, Tempe, AZ, USA
[b] School of Ocean and Earth Science and Technology, University of Hawaii, Honolulu, HI, USA
[c] Department of Geological Sciences, Michigan State University, East Lansing, MI, USA
[d] Research School of Earth Sciences, Australian National University, Canberra, Australia
[e] Smithsonian Institution, Museum Conservation Institute, Suitland, MD, USA

Received 13 September 2012; accepted in revised form 16 February 2013; available online 6 March 2013

Abstract

Nakhlite Miller Range (MIL) 03346 contains many secondary phases resulting from aqueous processes, including formation of poorly crystalline iddingsite-like veins in olivine, the precipitation of Ca-sulfates and Fe,K-sulfates from evaporating fluids, alteration of titanomagnetite to secondary Fe-oxides, and the dissolution of magmatic Ca-phosphates and residual glass in the mesostasis. A surprising variety of alteration products occur in association with olivine in MIL 03346, including: patches of incipiently-altered olivine, large Si-enriched olivine-hosted veins (up to 10 μm across) some of which are complex in morphology and are composed of several phases, small Fe,S(±K)-rich veinlets that crosscut the Si-enriched veins, Ca-sulfates filling cracks in olivine, and secondary Ca-phosphates. Elemental abundances and distributions in these alteration products are consistent with the mobilization of elements from readily dissolved phases in the mesostasis such as phosphates and residual glass. Under favorable weathering conditions, these phases dissolve more readily than pyroxenes, plagioclase, and even olivine at low pH. The occurrence (crosscut and devolatilized by the fusion crust) and composition of Si-enriched alteration veins in olivine are consistent with their formation on Mars. Si-enriched, poorly crystalline alteration products and secondary Ca-sulfates commonly occur in nakhlites, but the habit and composition of these alteration products differ between meteorites. Elemental distributions in these secondary phases suggest at least two episodes of alteration have affected MIL 03346, and subtle differences in secondary minerals and chemistry indicate that each nakhlite experienced its own unique alteration history either on Mars, Earth, or both. The variable Al content and range of morphologies of the olivine-hosted Si-enriched veins suggest variable alteration conditions consistent with a water-limited regime. If the secondary phases in MIL 03346 can be shown to have formed on Mars, their chemistry will provide important clues to the aqueous environments and processes at the time of their formation. However, elevated S and REEs, Ce anomalies, and association of secondary minerals with post-impact cracks and voids indicate that terrestrial weathering has significantly affected MIL 03346. This work highlights the difficulty in distinguishing pre-terrestrial aqueous alteration from later chemical weathering of susceptible mineral phases even in meteorites with limited terrestrial modification.

* Corresponding author. Address: LROC/ASU, P.O. Box 873603, Tempe, AZ 85287, USA. Tel.: +1 480 727 9484.
E-mail address: jstopar@asu.edu (J.D. Stopar).

0016-7037/$ - see front matter © 2013 Elsevier Ltd. All rights reserved.
http://dx.doi.org/10.1016/j.gca.2013.02.024

1. INTRODUCTION

The products of aqueous alteration processes that occur in nakhlite meteorites potentially provide important evidence of surficial environments during the last 1.3 billion years of martian history (Swindle and Olson, 2004) by reflecting the composition of the fluid, composition of the host rock, and the conditions of their formation. Sulfates, carbonates, halite, and iddingsite-like assemblages (e.g., Bridges et al., 2001; Treiman, 2005; Wentworth et al., 2005; Velbel, 2012) are phases identified as most likely formed on Mars. Nakhlite Miller Range (MIL) 03346 contains many products of aqueous alteration including Ca-sulfates and Si-enriched, poorly crystalline veins in olivine. While similar alteration products occur in the other nakhlites, the chemistry and habit of these products differ, suggesting local variations in conditions of alteration. Some secondary products are similar in composition to Antarctic, or other terrestrial alteration, and cannot currently be tied to a specific planet of origin. It is, therefore, important to study aqueous alteration products in martian meteorites, such as MIL 03346, to better understand their genesis and origin.

MIL 03346 is a nakhlite that was collected from Antarctica and has since been the subject of intense study (e.g., Dyar et al., 2005; Treiman, 2005; Day et al., 2006; Imae and Ikeda, 2007; Hallis and Taylor, 2011; Udry et al., 2012). MIL 03346 contains many secondary phases that have resulted from aqueous alteration processes, including poorly crystalline Si-enriched veins similar in composition to a combination of clay minerals and Fe-oxides (henceforth referred to as iddingsite-like) found in olivine, Ca-sulfates and Fe,K-sulfates precipitated from evaporating fluids, titanomagnetite altered to secondary Fe-oxides, and altered magmatic Ca-phosphates and residual glass in the mesostasis. Iddingsite-like alteration veins as well as Ca-sulfates have been identified in other nakhlites, and detailed chemical characterization of such alteration allows for comparison among these meteorites.

Bunch and Reid (1975) described a poorly crystalline brownish alteration product associated with olivine grains in Nakhla and Lafayette, possibly comprising montmorillonite plus chlorite and goethite. The term "iddingsite" has a variety of definitions and is often used to refer to any poorly crystalline Si-enriched mixture of olivine (or even pyroxene) alteration products. However, Eggleton (1984) and Smith et al. (1987) have given iddingsite a more specific definition as a mixture of smectite (i.e., saponite) and goethite. For the purposes of this research, we consider iddingsite to be a mixture of smectite-group minerals and Fe-oxides.

Olivine-hosted alteration in the nakhlites is generally depleted in Ca and K compared to terrestrial iddingsite (Bunch and Reid, 1975). Gooding et al. (1991) described iddingsite-like veins in Nakhla, enriched in Fe and Si and found primarily along fractures in olivine. These veins are truncated by the fusion crust and faulted by stress, implying a pre-terrestrial origin. These veins are also enriched in Cl, K, O, and Si compared to olivine and potentially hydrated. Some portions of olivine in Nakhla were described as being coated with a layer of poorly crystalline material, possibly smectite. In Lafayette, Treiman et al. (1993) described three types of olivine alteration products: coarse-grained phyllosilicates, fine-grained phyllosilicates, and "porous oxides" (possibly magnetite or maghemite). Governador Valadares also contains clay minerals mixed with hydrated Fe-oxides on the rims and in cracks of olivine (Berkeley et al., 1980).

Similar olivine-hosted alteration products are observed in all known nakhlites (Treiman, 2005; Velbel, 2012). Transmission electron microscope observations of the olivine-hosted alteration veins reveals lattice fringes consistent with smectite-group minerals in Nakhla (Gooding et al., 1991), Lafayette (Treiman et al., 1993; Changela and Bridges, 2011), NWA 817 (Gillet et al., 2002), and Yamato 00593 (Noguchi et al., 2009). Gillet et al. (2002) and Sautter et al. (2002) identified smectite in the veins of NWA 817 using Raman spectroscopy and X-ray diffraction. Imae et al. (2003) identified smectite-group minerals in Yamato 000593 by Fourier transform infrared spectroscopy; Treiman (2005) and Kuebler et al. (2007) also report iddingsite in the Yamato nakhlites. Noguchi et al. (2009) identified laihunite, a high temperature oxidation product, on the rims of olivine, which at the fusion crust, is decomposed to magnetite and amorphous silicate, implying a pre-terrestrial origin. Non-crystalline Fe–Mg–Al–Si material with a composition similar to smectite or serpentine volumetrically dominates the iddingsite-like vein assemblages in all five of the nakhlites examined by Changela and Bridges (2011). Hallis and Taylor (2011) recently described iddingsite-like alteration products in four Miller Range nakhlites that imply pre-terrestrial mobilization of a limited amount of Al at low pH. The presence of Fe-oxide veinlets toward the outside of these veins suggests increasingly oxidizing solutions over time. The olivine-hosted iddingsite-like alteration product in the nakhlites is generally depleted in Ca and enriched in K compared to terrestrial iddingsite (Bunch and Reid, 1975).

As minerals dissolve during aqueous processes, they decompose at different rates based upon the susceptibility of their crystal structure to react with the solution. Therefore, the distributions of soluble elements in rocks afford insight into processes and conditions of aqueous alteration. Chemical analysis of the aqueous alteration products in MIL 03346 is expected to improve our understanding of the genesis and origin of these products, a particularly valuable topic for meteorite finds. In addition, secondary phases in this meteorite that formed on Mars will provide important clues regarding the chemistry of martian waters and conditions of alteration. With this aim, we have combined laser-ablation inductively-coupled plasma mass spectrometry (LA-ICPMS), scanning electron microscopy (SEM), and electron microprobe point analyses and X-ray imaging to quantify and characterize elemental abundances, particularly trace elements, and their distributions in MIL 03346.

2. SAMPLES AND METHODS

In total, seven sections (,94 ,105 ,126 ,128 ,171 ,173 ,174) of MIL 03346 were studied using optical microscopy as well as backscattered scanning electron (BSE) imaging and

energy dispersive spectrometry (EDS) imaging techniques in order to assess variations in alteration throughout the meteorite. All sections were derived from the original processing of the meteorite. Thin sections ,94 ,105 ,128 ,173 and ,174 were derived from parent ,3 on the east face of the meteorite (McBride, 2007, personal communication; Righter and McBride, 2011). Thick sections ,173 and ,174 were derived from the ,166 section of parent ,3 from the east face of the rock (Satterwhite, 2011, personal communication). Thin section ,171 was produced from split ,23 from the outermost (fusion-crusted) portion of parent ,0. One section (,94) was analyzed by electron microprobe using the University of Hawaii Cameca SX-50 with wavelength dispersive spectrometry (WDS) for quantitative point analyses and elemental mapping. WDS mapping of the entire section for 10 elements (Al, Ca, Fe, K, Mg, Na, P, S, Si, and Ti) was completed at a voltage of 20 kV, current of 80 nA, per pixel dwell time of 12 μs, and pixel scale (spot diameter) of 15 μm. WDS quantitative point analyses were acquired using a 30 nA current, accelerating voltage of 15 kV, and 20 s peak time with 10 s of background. Electron microprobe data was reduced using the SAMx software package.

2.1. LA-ICPMS methods

A LA-ICPMS system (193-nm laser with adjustable spot diameter and repetition rates) at the Australian National University was used to determine the trace element abundances in olivine, clinopyroxene, bulk mesostasis, iddingsite-like veins, and other alteration products in MIL 03346. Two thick sections (,173 and ,174) were used for this analysis. Thick sections (>100 μm thick) were used to prevent the laser from ablating through the sample and into the glass slide.

A laser spot diameter of 70 μm and a repetition rate of 4–5 Hz were used for trace element point analysis on large mineral grains such as olivine and augite. Traverse analyses, where the sample moves in a straight line under the laser beam, were performed with a repetition rate of 10 Hz to collect bulk chemical information from the mesostasis because individual chemical phases are smaller than the spatial resolution. For olivine alteration products, a smaller spot diameter of 19 μm was used with a repetition rate of 3–4 Hz. 19 μm was the smallest available spot diameter for this instrument, and because many of the alteration products are smaller than 19 μm, measured elemental abundances represent mixtures of alteration products and host mineral (e.g., olivine).

The LA-ICPMS data were reduced to element concentrations following the procedure of Norman et al. (1996). Instrument sensitivity was calibrated using the NIST 612 glass, and each analysis was normalized to the concentration of an independently known element to compensate for variations in ablation efficiency between the mineral phases and the 612 reference glass (i.e., an internal standard). Thus, analyses were normalized to Ti (for titanomagnetite), the stoichiometrically calculated oxide CaO (for augite, olivine melt inclusions, mesostasis, and alteration products of these phases), and the calculated oxide SiO_2 (for olivine and its alteration products) concentrations determined by electron microprobe using thin section ,94. For plotting, the resulting REE abundances are normalized to mean CI chondrite abundances of Palme and Beer (1993) updated in Palme and Jones (2003). LA-ICPMS as a tool to study aqueous processes is useful, but several important tracers of alteration were not measured, including K (attributable to interference with argon gas), light elements such as H and S (attributable to high backgrounds and molecular interferences), and negative ions such as Cl^- (attributable to low yield of negative ions). Mercury signals were below detection limits as were, generally, Th and U, two elements whose fractionation can reflect martian weathering processes (e.g., Taylor et al., 2006). This technique is, however, sensitive to light rare earth element (LREE) enrichments and Ce anomalies, which can result from terrestrial aqueous alteration of meteorites (e.g., Mittlefehldt and Lindstrom, 1991; Crozaz and Wadhwa, 2001; Crozaz et al., 2003; Wadhwa et al., 2004). These fractionations result from the slight differences in ionic potential and mobility of LREEs compared to heavy rare earth elements (HREEs) and Ce^{4+} compared to Ce^{3+}, discussed further below.

Uncertainty in LA-ICPMS data can be described in terms of relative standard deviation (RSD; i.e., the standard deviation divided by the mean, expressed as a percentage) (Norman et al., 1996, 2004). The small laser diameter and slow repetition rates used for this study resulted in reduced precision compared to some previous studies. Some trace elements, particularly REEs in olivine, have concentrations near or below detection limits and, thus, intrinsically low precision. Detection limits range from 0.032–0.826 ppm for point analyses of olivine. For this study, replicate analyses of the NIST 612 glass reproduced within 10% at 3 Hz and spot diameter 19 μm; 7% at 5 Hz and spot diameter 19 μm; and 7% at 4 Hz and 70 μm. For REEs, NIST 612 glass is reproduced within 7% at 3 Hz and spot diameter 19 μm; 3% at 5 Hz and 19 μm; and 2% at 4 Hz and 70 μm. Reported P_2O_5 abundances have the largest uncertainty resulting from high background owing to molecular interferences from $^{15}N^{16}O$ with ^{31}P.

The internal standardization to a specific CaO, SiO_2, or Ti abundance from another section of the same meteorite results in a small amount of uncertainty for complex and poorly crystalline phases (i.e., alteration products), and the calculated abundances are based on a best estimate determined by electron microprobe point analyses. For the olivine-hosted veins, the average electron microprobe SiO_2 abundance of 42.4 wt.% was used for normalization. In some cases, the olivine-hosted vein material was smaller than the laser spot size. However, in all cases less than an estimated 10% of the ablated volume was host olivine or void space rather than alteration product (equivalent to ~41.5 wt.% SiO_2), adding ~2% uncertainty to the absolute trace element abundances as a result of the relatively small size of the olivine-hosted veins. Relative abundances will be less affected by this uncertainty, especially when the element of interest is below detection limits in olivine.

Concentrations of CaO and SiO_2 were determined by electron microprobe for the major phases: augite and olivine. Bulk mesostasis and olivine melt inclusions are,

however, fine-grained mixtures of an assemblage of minerals and the elemental abundances may differ considerably. Normalizations of bulk mesostasis and olivine melt inclusions were performed using average values of CaO (5.5 wt.%) determined by electron microprobe analyses of similar materials in section ,94.

2.2. Data collection strategy

LA-ICPMS elemental abundances were determined for a variety of minerals and alteration products in MIL 03346 in order to fully characterize both the primary and alteration phases. To this end, nine point analyses were acquired from the interior portions of augite and one from an altered augite with a brownish coloration and weathered appearance. Three traverses were made within the mesostasis with the objective of collecting a bulk analysis representing all of the phases in the interstitial areas including titanomagnetite and Fe-rich olivine. These traverses are referred to here as bulk mesostasis. The analysis "Meso Fayalite" was centered on a relatively large Fe-rich interstitial olivine; however, there is some mixing with the surrounding mesostasis. Three additional analyses "meso TM" were centered on relatively large dendritic titanomagnetites in the mesostasis, again with some mixing with the surrounding mesostatis.

Only one large cumulate olivine phenocryst is available for characterization in each thick section. LA-ICPMS analyses were collected from six points in unweathered olivine cores, two from the Fe-rich rims, and two from moderately altered patches in olivine. Another 11 points were collected from the iddingsite-like veins that include smaller Fe,K,S-rich materials. Most of the olivine-hosted iddingsite-like veins are somewhat smaller than the laser spot, and therefore, these analyses represent mixtures of "vein + olivine". We expect the trace element signatures, especially the REEs of these olivine-hosted alteration veins, to be dominated by the trace element abundances in the veins because olivine typically has very low REE abundances. An additional three point analyses were collected from a single melt inclusion in the cumulate olivine (referred to as Inclusion 1.1, 1.2, and 1.3).

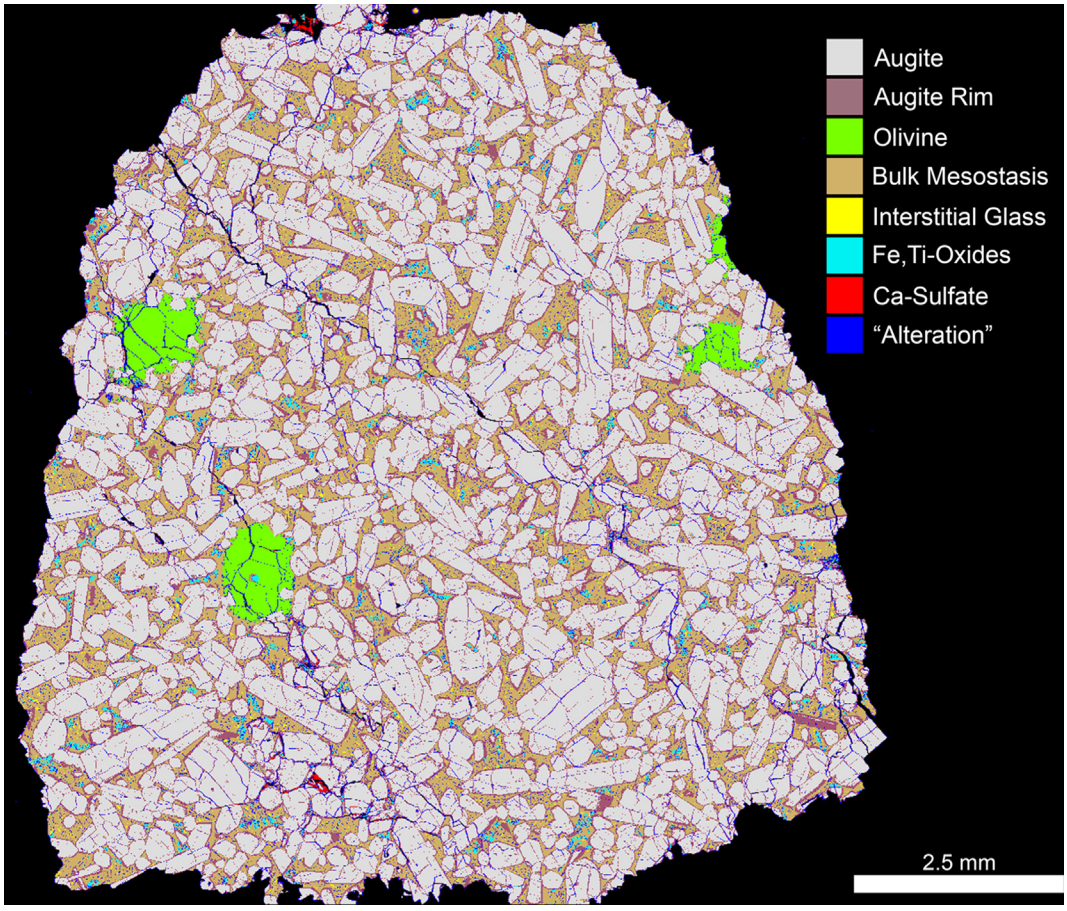

Fig. 1. Mineral map of nakhlite MIL 03346,94 derived from 10 electron microprobe element maps (scale is 15 μm/pixel). Pyroxene (augite) is shown in light purple and the iron-rich rims in dark purple. Augite and its rims account for 80.6% by area, olivine (green) occupies 2.7%, and mesostasis (brown) is 16.0% of this thin section. Interstitial silica glass (yellow) is 0.8% of the total thin section and Fe,Ti-oxides (cyan) account for 1.4%. Ca-sulfates (red) are a minor component at 0.07%, and other alteration (blue) found along cracks throughout the thin section, as veins in olivine and as patchy alteration in the interstitial groundmass amounts to 0.72%. (For interpretation of the references to colour in this figure legend, the reader is referred to the web version of this article.)

Table 1A
Mineral modes for MIL 03346 (vol.%).

	This study	Imae and Ikeda (2007)	Dyar et al. (2005)	Day et al. (2006)	Hallis and Taylor (2011)	Udry et al. (2012)[c]
Pyroxene	80.6	67.7	70.8	78.4	78.3	78.3
Olivine	2.7	0.8	2.8	1.1	2.9	2.9
Mesostasis	16.0	31.5	26.2	19.8	17.4	17.4
Alteration	0.79[a]	Not reported	0.2[b]	0.24[b]	<0.5[a]	<0.5[a]

[a] Includes "iddingsite" and Ca-sulfate.
[b] Only includes "iddingsite".
[c] Weighted average of paired meteorites.

Table 1B
Modal comparison to other nakhlites (vol.%).

	Pyroxene	Olivine	Mesostasis	Alteration
MIL 03346[a]	80.6	2.7	16.0	0.79
Nakhla[b]	80.8	10.8	8.4	Not reported
Lafayette[b]	73.5	16.7	9.8	Not reported
Gov. Val.[b]	81.2	8.9	9.8	Not reported
Y000593[c]	76.7	12.2	11.1	Not reported
NWA 998[d]	77.6	9.2	13.2	Not reported
NWA 817[e]	69	10	20	Not reported

[a] This study.
[b] Freidman Lentz et al. (1999).
[c] Imae et al. (2003).
[d] Treiman and Irving (2008).
[e] Sautter et al. (2002).

Electron microprobe and scanning electron microscope (SEM) point analyses and elemental maps were also collected as needed to study major and minor elements and their distribution in both the primary minerals and alteration products. A mineral phase map was created using the ENVI software package for image analysis (Fig. 1). This map was created by stacking individual electron microprobe X-ray elemental maps into a single image and using ENVI's built in spectral classification tool to identify pixels belonging to each mineral class (following the techniques of Hicks, 2002), which are then color-coded accordingly. From this map, the modal abundance of each mineral phase is determined.

The uncertainty associated with this mineral classification technique is not well quantified, though Hicks (2002) did compare the mineral modes acquired by this technique to those calculated by other methods and found agreement within a few volume percent. Here, we find good agreement with the mineral modes calculated by other researchers for this meteorite despite the inherent differences in mineral abundances among different thin sections (Table 1A). The most important factor in acquiring accurate mineral modes is the selection of representative "spectral" classes for all the minerals present at the resolution of the element maps (in this case >15 μm). At this resolution, many small alteration veins are not resolved, nor are fine-grained mesostasis minerals such as Ca-phosphates or feldspars. Fortunately, many the larger Si-enriched olivine-hosted veins and void-filling sulfate products are resolved and can be spectrally identified based upon ratios of Si, S, Fe, Ca, and Mg.

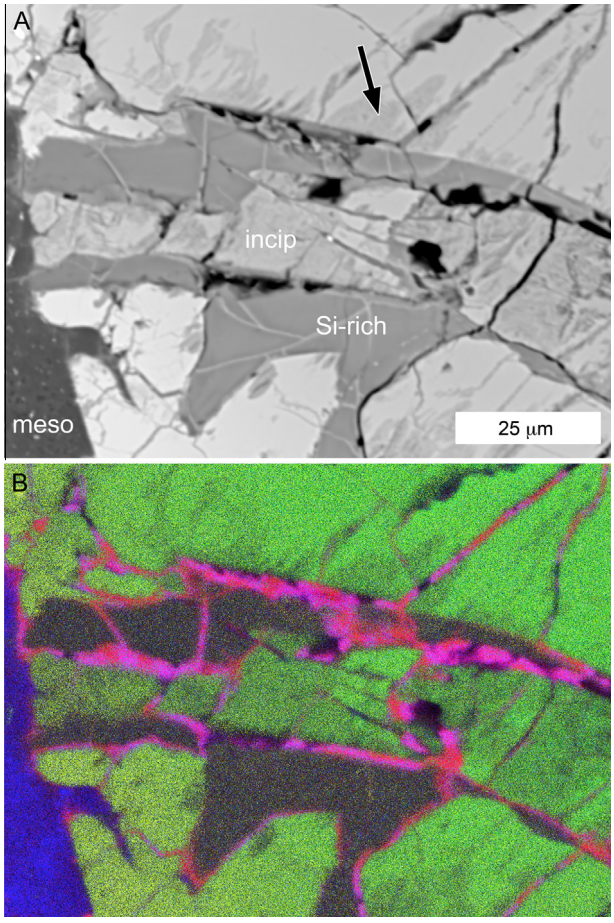

Fig. 2. Incipient alteration and alteration veins in olivine (MIL 03346,94). (A) SEM backscattered electron image (BSE) of alteration in olivine. (B) 4-element BSE false-color image (blue = K, green = Mg, yellow = Fe, and red = S). Olivine (yellow-green) is incipiently-altered in patches along the edges of veins and has a channelized texture ("incip" and black arrow). These areas are depleted in Fe and Mg. The dark veins ("Si-rich") are Si-enriched and even more depleted in Fe and Mg. Red veinlets crosscutting the larger Si-enriched veins are rich in S. Magenta veinlets are rich in both K and S; some of these veinlets may be jarosite. (For interpretation of the references to colour in this figure legend, the reader is referred to the web version of this article.)

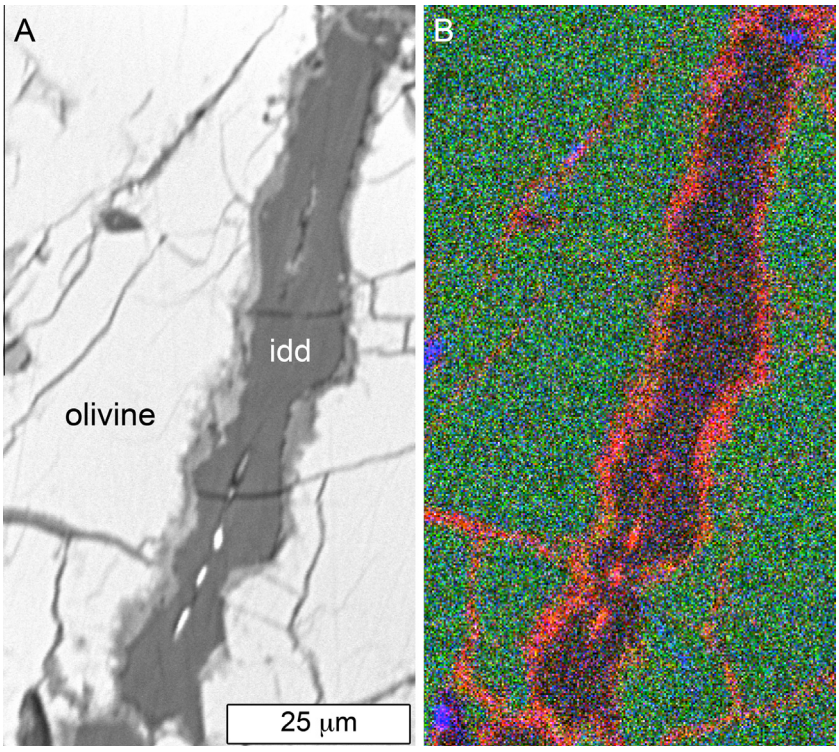

Fig. 3. Alteration vein in olivine with complex morphology and multiple phases (MIL 03346,105). (A) SEM backscattered image (BSE) of a large olivine-hosted vein ("idd") with morphologic similarities to terrestrial iddingsite. (B) SEM 3-element false color image (red = S, green = Fe, and blue = Ca). The core of the vein is Si-enriched, and the edges of the vein are Fe,S,K-rich (possibly jarosite). (For interpretation of the references to colour in this figure legend, the reader is referred to the web version of this article.)

3. RESULTS

The igneous petrography of MIL 03346 has been discussed in depth elsewhere (Dyar et al., 2005; Treiman, 2005; Day et al., 2006; Imae and Ikeda, 2007; Hallis and Taylor, 2011; Udry et al., 2012); therefore, we discuss igneous mineralogy only as it relates to our study. The mineralogy is similar to that of other nakhlites, except that the fine-grained mesostasis is more abundant and olivine phenocrysts are less abundant (Table 1B). MIL 03346 has the lowest modal abundance of olivine of any of the nakhlites (Treiman, 2005; Day et al., 2006; Hallis and Taylor, 2011; Udry et al., 2012), here totaling ~2.7 vol.%. Olivine is present both as mm-scale phenocrysts and as small grains in the mesostasis. Olivine phenocrysts are $\sim Fo_{43}$ with iron-rich rims that range from Fo_{33} to Fo_{10} and account for ~0.8% of the meteorite. Interstitial olivine is $\sim Fo_6$. Olivine phenocrysts are host to magmatic inclusions that contain a wide variety of fine-grained minerals. There is a surprising variety of alteration products associated with olivine in MIL 03346 (e.g., Figs. 2 and 3): (1) patches of incipiently-altered olivine, (2) large Si-enriched veins some of which have multiple phases and complex morphology, (3) small Fe,S(±K)-rich veinlets that crosscut the Si-enriched veins, (4) S-enriched phases filling cracks in olivine, and (5) secondary Ca-phosphates.

The most abundant phase is augite and accounts for ~80%, by area, of the meteorite (Table 1; Fig. 1). These clinopyroxenes have magnesian cores and Fe-rich rims. Some of the clinopyroxenes contain alteration products including alteration veins and Ca-sulfates.

The second most abundant phase is mesostasis (~16%), which is actually a fine-grained mixture of numerous minerals: plagioclase, Fe,Ti-oxides such as titanomagnetite, sulfides, phosphates, silica-rich glass, limited alkalic feldspars, and various alteration products. There are patchy areas of alteration in the mesostasis, where titanomagnetites have been converted to low-Ti magnetite (Day et al., 2006), and the fine-grained mineralogy has been altered. Interstitial silica glass is ~0.8% of the meteorite and Fe,Ti-oxides ~1.4%. Locally, there are alteration veins in the mesostasis as well as Ca-sulfates that fill cracks and void spaces. Ca-sulfates are a minor component ~0.07% of the meteorite, but abundance varies with location in the meteorite and from section to section (e.g., Velbel et al., 2010; Hallis et al., 2011; Hallis and Taylor, 2011). Fries et al. (2006) first identified jarosite as crack-filling material in MIL 03346, later confirmed by Vicenzi et al. (2007a,b) and Kuebler et al. (2007). In addition, some sections show clear evidence of terrestrial alteration along the edges of the meteorite (Fig. 4). Total alteration is estimated at less than 1 vol.% of the meteorite.

Incipiently-altered olivine (Fig. 2) typically has a channelized texture similar to some small *en echelon* etch textures described in terrestrially weathered olivine (Velbel, 2009; his Fig. 5) and appears darker than unaltered olivine in backscattered electron images. Elemental X-ray images show enrichments of Al, Si, P, S, and K in incipiently-al-

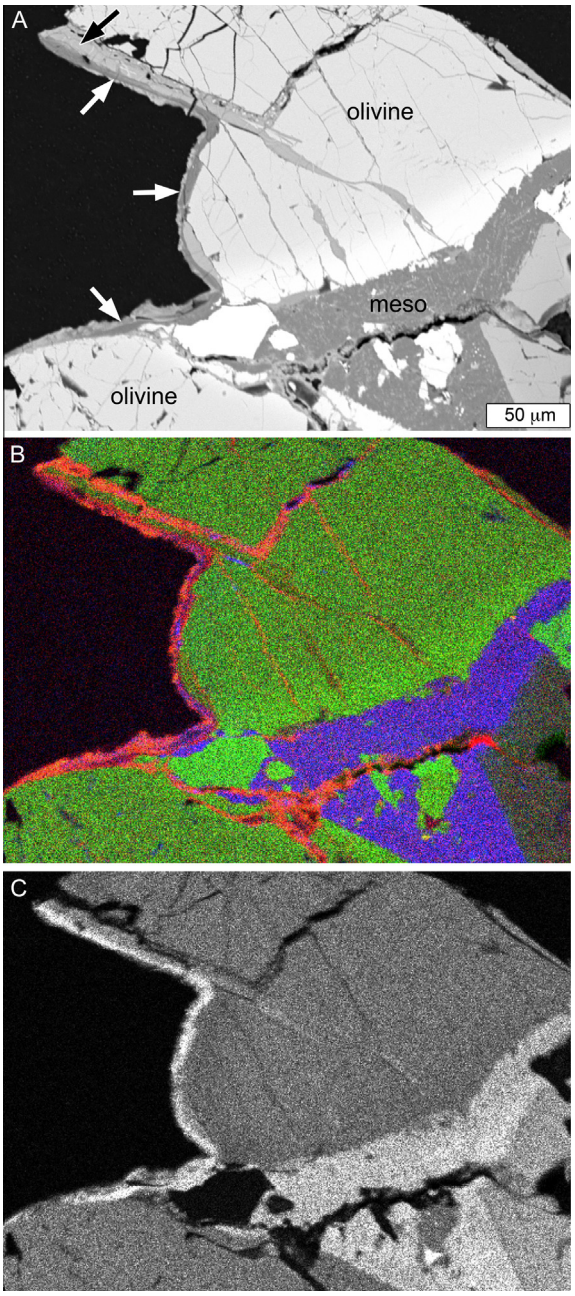

Fig. 4. Olivine alteration at an Antarctic weathering surface on MIL 03346,126. (A) SEM BSE image of part of an olivine phenocryst with an Fe-rich rim that is located along the edge of the thin section. A pre-terrestrial Si-enriched olivine-hosted alteration vein is truncated by the edge of the section (black arrow) and is coated by an outer layer (white arrows) interpreted as an Antarctic weathering surface. (B) SEM 3-element false color image (red = S, green = Fe, and blue = Al) shows that the outer layer is enriched in Al and S. Fe is depleted at the edge, as is Ca (not shown). S and K are often correlated along the edge and in cracks and veins throughout the olivine and mesostasis ("meso"). C) SEM Si elemental map showing a Si-enrichment corresponding to the Antarctic weathering surface. (For interpretation of the references to colour in this figure legend, the reader is referred to the web version of this article.)

tered areas of olivine compared to the unaltered cores and are depleted in Mg, Ca, Fe, and Mn (Fig. 2). Olivine-hosted alteration veins are further depleted in Fe and Mg and enriched in Si compared to unaltered olivine and the patches of incipient alteration (Table 2; Fig. 5). Therefore, the patches of incipient-alteration are interpreted as areas of partial olivine dissolution and/or corrosive replacement at etch pit-like interfaces. Fig. 5, which compares Mg, Fe, Al, S, and Si oxide abundances in olivine, incipiently altered olivine, and olivine-hosted veins, illustrates that the patches of incipient alteration consist of olivine replacement phases enriched in Si with minor Al, but depleted in Fe and Mg compared to the surrounding olivine with further Si enrichments and Fe and Mg depletions occurring in the olivine-hosted veins.

Olivine appears more heavily altered in some sections compared to others. For example, in several sections of MIL 03346 (Figs. 3, 6 and 7), rhombic patterns resembling terrestrially weathered olivine etch-pits (e.g., Velbel, 2009) suggest the initial stages of iddingsite formation (e.g., Smith et al., 1987). Such textures are known from terrestrial olivine subjected to aqueous alteration; for example, a serpentinized olivine from the Laurel Creek Complex, Georgia, shows rhomboid-bounded phyllosilicate and serpentine venation with incipiently corroded olivine at the vein margins (Fig. 8). In some cases (Fig. 6), complex rhomboid-bounded Si-enriched veins in MIL 03346 are contained within altered olivine; in others (Fig. 7) these precipitates have a simpler morphology, lack serrated margins, and are spatially separated from incipiently altered olivine and each other (at least in the two dimensions represented by the sections). There are three morphological features associated with many of the more complex forms of these veins (Fig. 3): a central veinlet that runs along the medial axis of the vein, a vein core that comprises the bulk of the interior of the feature ("idd" in Fig. 3), and an outer phase with a poorly defined boundary that appears to extend out into the olivine. In some of these complex veins, the central veinlet is Fe-rich with lesser S, while the outer rind is Fe,K, and S-rich, suggesting a jarosite component in the assemblage. In the more simple form (Fig. 7), both the central veinlet and the S-rich outer phase are absent. Iron-oxides are not apparent at the resolution of a few microns and, if present, must be poorly crystalline. Some of these alteration veins become vesicular within a few hundred microns of the fusion crust indicating thermal metamorphism and devolatilization of these veins during the passage of MIL 03346 through the Earth's atmosphere and confirming their pre-terrestrial origin (Fig. 9).

The second most obvious alteration products in MIL 03346 are the Ca-sulfate precipitates scattered in cracks and voids throughout the meteorite. Hallis and Taylor (2011) observed that these phases are concentrated near terrestrially weathered surfaces, and Fig. 10 shows Ca-sulfates associated with Antarctic weathering products crosscutting vesiculated fusion crust at the meteorite's surface (see also Velbel, 2012, his Fig. 3). The chemistry of the Ca-sulfates found in the meteorite interior is consistent with anhydrite or bassanite, but the original hydration state of the Ca-sulfates is uncertain at this time as a result of the potential

Table 2
Electron microprobe olivine chemical compositions.

	Unaltered olivine core[a]		Unaltered olivine rim[a]		Incipiently-altered olivine[b]		Olivine-hosted vein[c]	
	wt.%	Detection limit	wt.%	Detection limit	wt.%	Detection limit	wt.%	Detection limit
SiO_2	33.5 ± 0.2	0.07	30.9 ± 0.7	0.07	37.7 ± 4.8	0.07	42.4 ± 1.5	0.07
TiO_2	*	0.05	*	0.05	*	0.05	*	0.05
Al_2O_3	*	0.05	*	0.06	0.44 ± 0.66	0.05	0.10 ± 0.03	0.05
Cr_2O_3	*	0.07	*	0.05	*	0.06	*	0.07
FeO	45.0 ± 0.3	0.08	58.1 ± 3.8	0.09	42.4 ± 5.0	0.08	37.8 ± 1.7	0.08
MnO	0.93 ± 0.04	0.06	1.4 ± 0.2	0.07	0.84 ± 0.22	0.06	0.63 ± 0.11	0.06
MgO	18.8 ± 0.2	0.04	7.6 ± 3.2	0.04	6.4 ± 3.4	0.04	3.1 ± 0.2	0.04
CaO	0.54 ± 0.02	0.03	0.37 ± 0.18	0.03	0.44 ± 0.33	0.03	0.14 ± 0.01	0.03
Na_2O	*	0.05	*	0.06	*	0.05	*	0.05
K_2O	*	0.03	*	0.04	0.23 ± 0.26	0.04	*	0.03
P_2O_5	0.11 ± 0.02	0.08	0.12 ± 0.03	0.08	0.38 ± 0.11	0.08	*	0.08
SO_3	*	0.09	*	0.09	1.3 ± 1.1	0.09	1.0 ± 0.4	0.09
Sum	98.83		98.44		90.01		85.25	
	$Fo_{42.6}$		$Fo_{18.7}$					

* Below detection limits.
[a] Average of 10 analyses, normalized to four oxygens.
[b] Average of nine analyses, normalized to four oxygens.
[c] Average of five analyses, normalized to four oxygens.

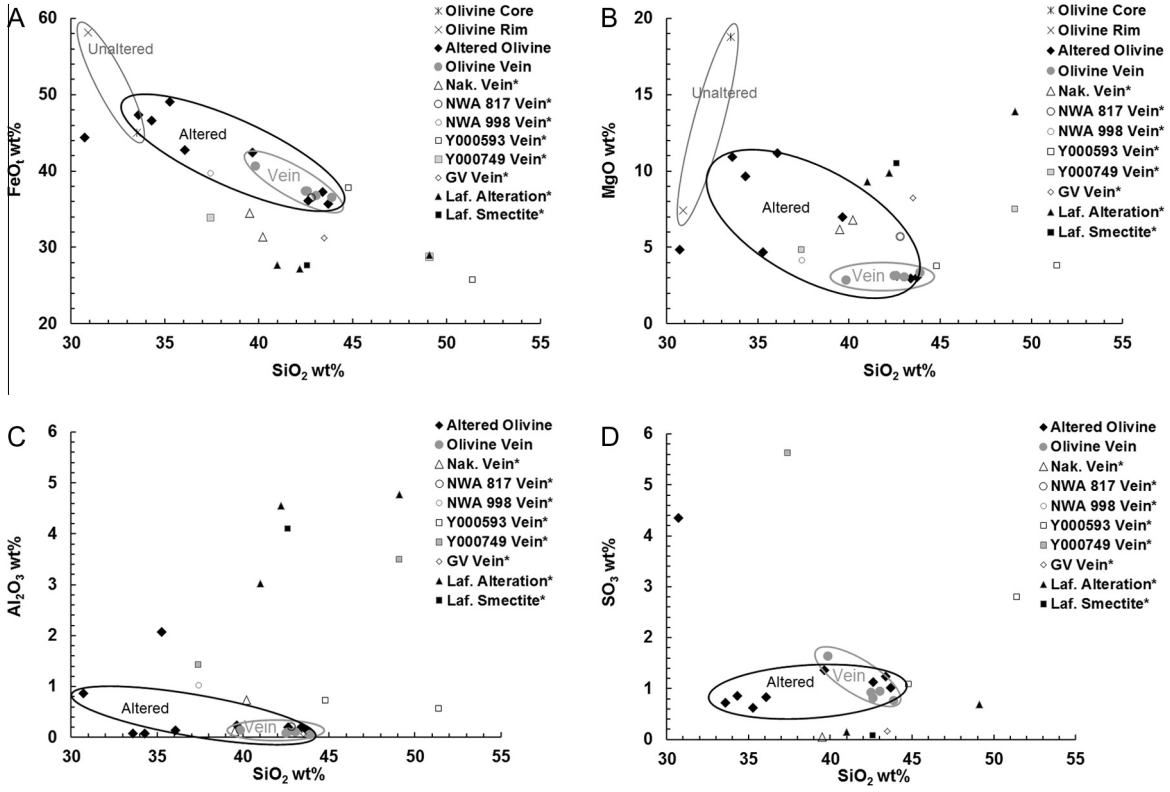

Fig. 5. Selected variation diagrams for olivine and alteration products in nakhlites. (A) FeO_t/SiO_2, total Fe is plotted as FeO, (B) MgO/SiO_2, (C) Al_2O_3/SiO_2, and (D) SO_3/SiO_2 ratios. *Nakhla olivine-hosted veins are average of 78 from Gooding et al. (1991) and average of 13 from Changela and Bridges (2011); NWA 817 olivine-hosted vein is average of 25 from Gillet et al. (2002); NWA 998 olivine-hosted vein is average of 3 from Treiman and Irving (2008); Y000593 vein from Noguchi et al. (2009) and average of 9 from Changela and Bridges (2011); Y000749 vein is from Treiman and Goodrich (2002) and average of 17 from Changela and Bridges (2011); Governador Valadares (GV) vein is average of 4 from Changela and Bridges (2011); Lafayette alteration is average of 83 from Treiman et al. (1993), average of 29 from Kuebler et al. (2004), and Changela and Bridges (2011); Lafayette smectite from Changela and Bridges (2011) are also plotted for comparison.

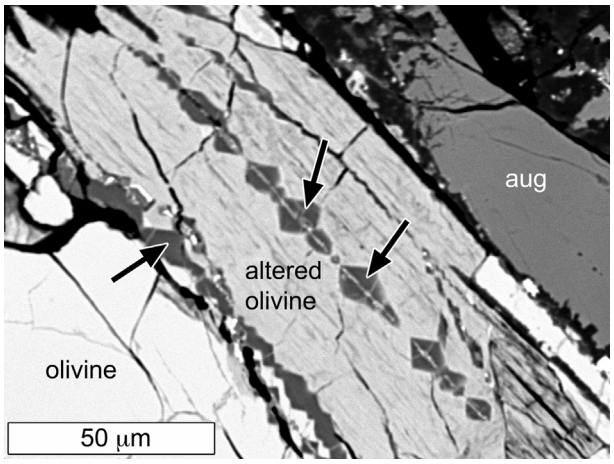

Fig. 6. Iddingsite-like vein morphology in MIL 03346,128 olivine. SEM backscattered electron image of vein with rhomboid-bounded serrations (black arrows) that resemble typical olivine etch-pits and is spatially associated with altered olivine (lower Z-contrast than olivine). The rhomboid-bounded serrations are enriched in Si and Ca with minor Al, and are depleted in Fe and Mg compared to the surrounding olivine. The altered olivine is adjacent to augite (aug) and mesostasis (meso). There are no S,K-rich outer bounding materials as in Fig. 4.

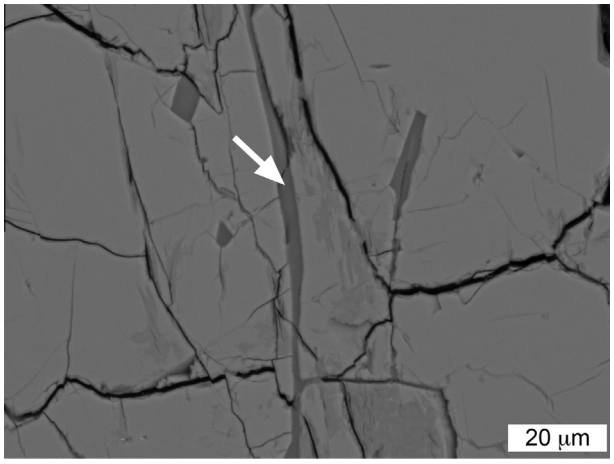

Fig. 7. SEM backscattered electron image of olivine alteration products in MIL 033463,171 including Si-enriched vein with simple morphology (white arrow), rhomboid-bounded Si-enriched precipitates, and altered olivine (lower Z-contrast patches). The rhomboid-bounded precipitates and the Si-enriched vein are spatially independent of one another and of the altered olivine material.

hydration/dehydration of sulfates (e.g., Gooding, 1978; Robertson and Bish, 2007) on Mars, during transit to Earth, in Antarctica, or while in storage.

3.1. Trace elements

LA-ICPMS analyses including phases, number of points, element abundances and RSDs are summarized in Table 3. Phases (and mixtures) with large RSDs reflect phases with heterogeneous composition. To create aqueous

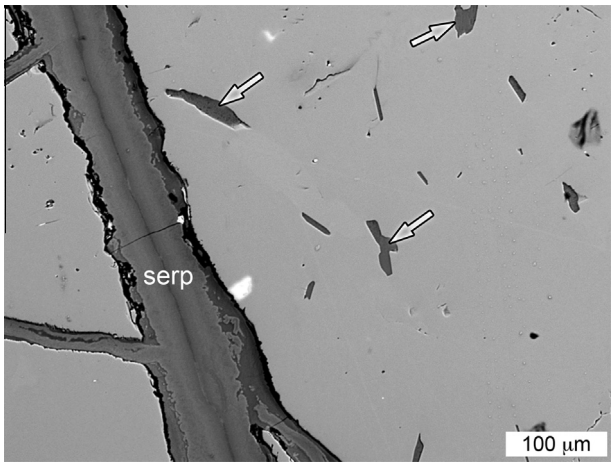

Fig. 8. Weathered serpentinized olivine of Laurel Creek Complex, northeast Georgia, U.S.A. Rhomboid-bounded phyllosilicate in olivine (arrows), meshwork serpentine venation of olivine ("serp"), and incipiently corroded olivine at vein margins.

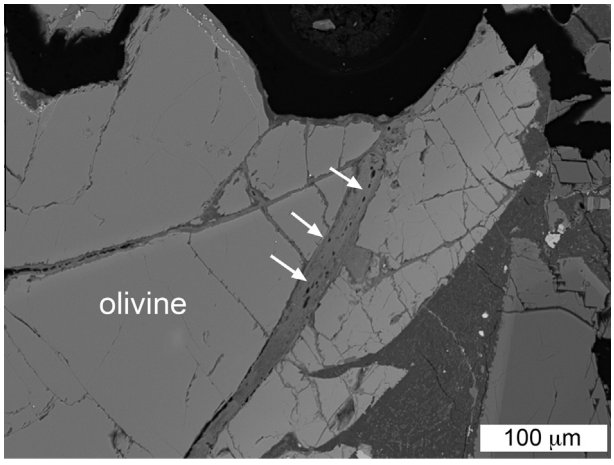

Fig. 9. Olivine-hosted alteration veins in MIL 03346,171 are vesicular (white arrows) within a few hundred microns of the fusion crust (just above top of image), consistent with thermal metamorphism and devolatilization of pre-terrestrial veins during the fusion crust formation in the Earth's atmosphere.

mobility plots (Fig. 11), we applied a whole rock normalization to minimize the effects of Cs, Rb, Pb, and Zn volatility and the potential loss of elements such as Co during core formation, which can be an issue with chondrite-normalized values. The whole rock value was calculated as the average of the values in Barrat et al. (2006) and Day et al. (2006). The mobility of an element in solution is typically evaluated by normalizing to an "immobile" element such as Ti. However, owing to the uncertain mobility of Ti, or any other typically immobile element, in MIL 03346 under either martian or terrestrial weathering conditions, we plotted elements according to their ionic potential, as a proxy for solubility, and normalized to whole rock values rather than to Ti. The aqueous solubility of an element is, in part, related to the ionic charge and radius of an ion

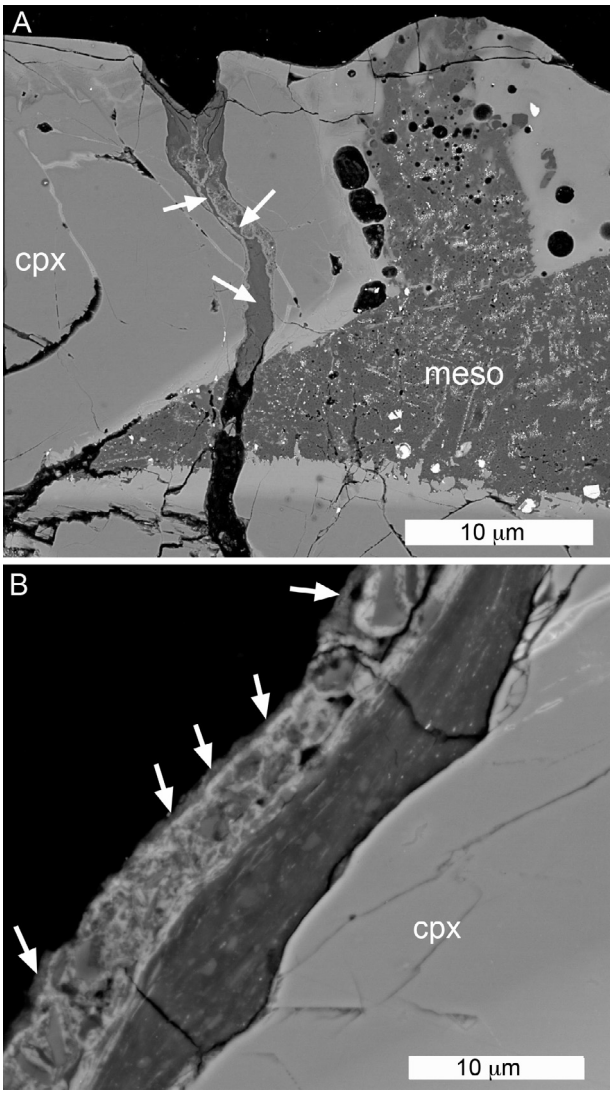

Fig. 10. Distribution of Ca-sulfates (white arrows) associated with the Antarctic weathering surface of MIL 03346,171 (SEM BSE). (A) Ca-sulfates precipitated in an Antarctic weathering vein near the surface of the meteorite. (B) Ca and S concentrated on the outermost portion of the Antarctic weathering surface.

(and thus ionic potential), and those with low ionic potential, such as Na^{+}, or high ionic potential, such as S^{+6}, tend to be more soluble; however, mobility of an element in solution is controlled by many other factors including pH, Eh, and other elements in solution (e.g., Loughnan, 1969, p. 51).

The whole-rock normalized abundances for olivine-hosted alteration veins show that the veins are enriched in some elements – Cs, Rb, Na, Ba, Pb, Sr – compared to unaltered olivine (Fig. 11), suggesting that these elements were mobile in solution. Whole rock Cs, Rb, Ba, and Pb are concentrated in the mesostasis phases as expected for incompatible lithophile elements. Sr and Na are found in both the bulk mesostasis and to some extent augite.

Phosphorus in the olivine-hosted veins appears elevated with respect to unaltered olivine (Fig. 11); however, the experimental uncertainty in determining P_2O_5 is relatively large. Rare secondary Ca-phosphates are consistent with the mobility of phosphorus in MIL 03346; however, they may be terrestrial in origin. Possible meteoritic sources for phosphorus include dissolved phosphates or interstitial glass. Olivine phenocrysts and augite are probably not significant contributors of phosphorus. Furthermore, olivine melt inclusions do not show any clear differentiations attributable to aqueous alteration and are probably not, therefore, a significant source of phosphorus to solution. Inclusion 1.3, however, is strongly enriched in Cs and Rb compared to other analyses of inclusions, demonstrating significant elemental heterogeneity over short distances in these inclusions. The abundances of elements, such as Ga, Cr, and Ti, in the olivine-hosted veins are generally low and may be only slightly enriched over unaltered to incipiently altered olivine, consistent with the general immobility of these elements (Fig. 11).

3.2. Rare earth elements, Pb, and Th

In unaltered olivine cores, most REEs were below detection limits and the overall abundance of REEs is low (Fig. 12). As olivine alters, the LREEs are particularly enriched, and Pb and Th are sometimes detectible. In the olivine-hosted veins, the REEs are generally enriched in addition to Pb and Th, implying at least some aqueous solubility of these elements. The bulk of the whole rock Pb and Th is located in residual mesostasis phases, a potential source for these elements in solution. Our REE patterns are generally consistent with those from other nakhlites (Treiman and Lindstrom, 1997; Bridges and Grady, 1999, 2000; Gillet et al., 2002; Wadhwa et al., 2004) and with the results of Day et al. (2006) (Fig. 13).

Mesostasis in MIL 03346 is enriched in LREEs (Fig. 13), as it is for other nakhlites. This LREE-enrichment is inherited from magmatic processes (Wadhwa and Crozaz, 1995; Treiman, 2005) rather than from fractionation of REEs during aqueous alteration. The other main carrier of REEs in the mesostasis is Ca-phosphate. The Ca-phosphates, only a few microns in length, are too small to be spatially resolved by LA-ICPMS and are a minor component (<1%) of the mesostasis, but they can account for 50% or more of the total REE budget. In nakhlites, apatite REE abundances are ~100–1000 times that of CIs (Wadhwa and Crozaz, 1995, 2003).

Augite REE patterns and abundances (Fig. 14) are consistent with the results of Day et al. (2006). Compared to the augite cores, which have stronger depletions of the lightest REEs, one brownish altered augite is greatly enriched in LREEs and has a larger negative Eu anomaly than unaltered augite cores.

Ce anomalies are calculated as the ratio of the measured chondrite-normalized Ce abundance to the interpolated Ce abundance (Ce^{*}) from adjacent La and Pr chondrite-normalized abundances. A value of 1 is equivalent to no Ce anomaly. The RSDs of La, Ce, and Pr for the LA-ICPMS standards is ⩽3.5%, whereas the RSD% of ~60–72% reported in Table 3 for the average of the olivine-hosted veins indicates that the La, Ce, and Pr abundances are heterogeneous in the points analyzed. Therefore, we consider Ce

Table 3
LA-ICPMS element abundances for various phases in MIL 03346 and calculated relative standard deviation (RSD).

Phase(s)	Olivine core		Olivine rim		Altered olivine		Olivine-hosted vein		Melt inclusion		Augite core		Altered augite	Bulk mesostasis		Meso fayalite	Meso TM	
Number of analyses	6		2		2		11		3		9		1	3		1	3	
Average abundance	wt.%	RSD	wt.%	RSD	wt.%	RSD	wt.%	RSD	wt.%	RSD	wt.%	RSD	wt.%	wt.%	RSD	wt.%	wt.%	RSD
Na_2O	0.01	*33*	0.01	*43*	0.09	*88*	0.17	*58*	0.48	*75*	0.26	*6.3*	0.73	5.3	*17*	2.0	0.09	*60*
MgO	20.1	*5.7*	12.6	*55*	22.0	*9.0*	12.8	*24*	1.4	*71*	15.4	*1.9*	9.1	0.90	*32*	1.1	0.20	*13*
SiO_2	33.5	*0*	31.1	*0*	37.7	*0*	42.4	*0*	21.8	*19*	52.2	*1.6*	74.5	67.6	*16*	36.9	1.8	*89*
P_2O_5	0.09	*97*	0.05	*78*	0.06	*30*	0.35	*47*	0.78	*31*	0.01	*38*	0.54	1.6	*14*	1.0	0.08	*34*
CaO	0.46	*5.4*	0.41	*1.7*	0.57	*1.3*	0.41	*19*	5.5	*0*	18.8	*0*	18.8	5.5	*0*	2.0	0.11	*14*
MnO	0.87	*5.3*	0.94	*21*	1.1	*4.0*	0.84	*14*	0.15	*18*	0.43	*2.8*	1.5	0.48	*36*	0.81	0.64	*3.2*
	ppm	RSD	ppm	RSD	ppm	RSD	ppm	RSD	ppm	RSD	ppm	RSD	ppm	ppm	RSD	ppm	ppm	RSD
Li	4.5	*32*	5.0	*76*	4.5	*32*	3.4	*43*	3.0	*59*	1.6	*7*	5.2	5.6	*52*	12	*	*
Sc	9.0	*13*	8.1	*13*	11	*6*	14	*9*	16	*12*	69	*3*	88	5.9	*23*	2.1	9.6	*22*
Ti	121	*18*	135	*45*	139	*21*	217	*20*	4781	*19*	1391	*9*	1379	6322	*30*	1843	119692	*0*
V	10	*13*	7.2	*38*	12	*11*	15	*14*	95	*15*	198	*6*	126	8.2	*29*	1.4	1676	*11*
Cr	68	*14*	24	*75*	56	*64*	90	*33*	31	*12*	2012	*15*	292	4.8	*40*	*	*	*
Co	114	*3.8*	93	*19*	132	*1*	77	*23*	26	*88*	36	*5*	55	14	*29*	21	37	*7.1*
Ni	184	*4.1*	100	*85*	188	*14*	123	*31*	40	*84*	62	*4*	28	3.0	*13*	1.7	5.8	*26*
Zn	147	*14*	194	*29*	153	*7*	154	*24*	44	*18*	36	*11*	174	88	*20*	133	727	*12*
Ga	0.22	*42*	*	*	0.18	*24*	1.2	*35*	9.5	*14*	2.3	*7*	7.0	24	*11*	9.4	48	*12*
Rb	*	*	*	*	0.18	*105*	4.3	*35*	79	*162*	*	*	8.8	15	*21*	8.1	5.0	*94*
Sr	0.28	*179*	*	*	0.51	*89*	14	*63*	73	*40*	26	*10*	612	640	*16*	235	11	*77*
Y	0.28	*39*	0.42	*51*	0.41	*3*	2.8	*34*	14	*19*	3.3	*9*	18	27	*14*	13	1.7	*33*
Zr	0.07	*54*	0.11	*19*	0.07	*6*	0.30	*43*	40	*13*	1.9	*19*	17	121	*5.2*	34	64	*5.8*
Nb	*	*	*	*	*	*	0.17	*75*	13	*67*	0.03	*18*	0.6	23	*13*	9.4	54	*23*
Cs	*	*	*	*	*	*	1.1	*30*	15	*163*	*	*	1.7	1.4	*36*	0.48	*	*
Ba	*	*	*	*	0.04	*15*	0.70	*55*	93	*107*	0.07	*90*	192	298	*19*	108	4.2	*75*
La	*	*	*	*	0.17	*106*	5.4	*61*	14	*65*	0.38	*29*	11	23	*14*	12	1.4	*125*
Ce	0.21	*116*	*	*	0.18	*93*	8.5	*51*	38	*79*	1.5	*22*	40	55	*12*	29	2.2	*98*
Pr	*	*	*	*	0.05	*92*	1.6	*65*	5.4	*83*	0.32	*15*	3.7	7.4	*12*	3.8	0.50	*64*
Nd	0.32	*41*	*	*	0.16	*81*	5.0	*61*	21	*81*	1.8	*16*	17	31	*12*	16	*	*
Sm	*	*	*	*	*	*	0.92	*50*	4.0	*72*	0.59	*17*	4.8	6.4	*11*	3.5	*	*
Eu	*	*	*	*	*	*	0.17	*27*	1.4	*60*	0.20	*24*	0.71	2.1	*8.5*	1.0	*	*
Gd	*	*	*	*	*	*	0.83	*53*	3.7	*56*	0.69	*16*	4.0	5.6	*14*	3.0	*	*
Dy	*	*	*	*	0.06	*9*	0.91	*35*	2.9	*36*	0.71	*8*	3.7	5.3	*13*	2.6	*	*
Ho	*	*	*	*	*	*	0.15	*60*	0.66	*23*	0.14	*11*	0.72	1.1	*18*	0.43	*	*
Yb	*	*	*	*	0.08	*14*	*	*	1.3	*13*	0.33	*30*	3.2	2.8	*15*	1.8	*	*
Lu	*	*	*	*	0.02	*25*	*	*	0.19	*11*	0.06	*21*	0.38	0.43	*21*	0.24	*	*
Hf	*	*	*	*	*	*	*	*	1.0	*24*	0.11	*41*	0.81	3.3	*8.3*	0.68	2.4	*37*
Pb	*	*	*	*	*	*	1.3	*61*	1.4	*47*	*	*	1.3	4.7	*20*	2.5	1.5	*59*
Th	*	*	*	*	*	*	*	*	0.79	*15*	*	*	0.68	2.7	*9.8*	1.0	*	*
U	*	*	*	*	*	*	*	*	0.22	*3*	*	*	*	0.55	*9.3*	*	*	*

* Below detection limits.

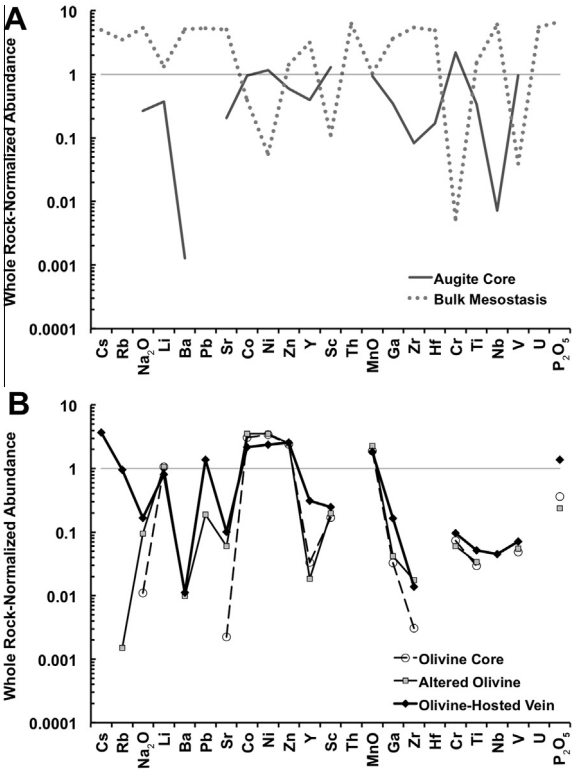

Fig. 11. Element mobility plot for major phases and alteration products in MIL 03346. LA-ICPMS abundances have been normalized to an average whole rock abundance calculated from Barrat et al. (2006) and Day et al. (2006). The elements with the lowest ionic potential are on the left, and the ionic potential increases to the right. (A) Bulk mesostasis and augite. (B) Unaltered olivine, incipiently altered olivine, and olivine-hosted veins.

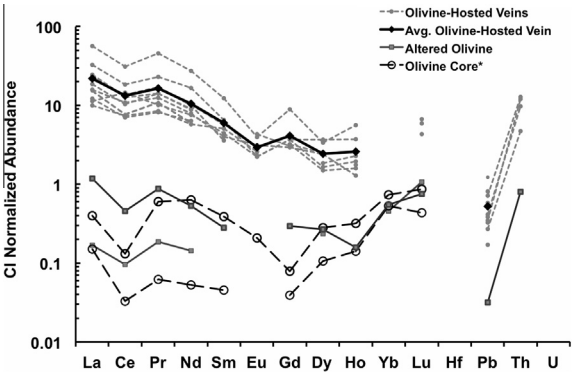

Fig. 12. Chondrite-normalized REEs in olivine, altered olivine, and Si-enriched olivine-hosted alteration veins in olivine. *Representative olivine cores from Day et al. (2006) are also plotted for comparison. Day et al. noted their olivine analyses are anomalously enriched in LREEs and have Ce anomalies, which might suggest some terrestrial contamination. REEs in unaltered olivine were below detection limits in this study.

anomalies (reported as Ce/Ce^*) with values 0.8–1.2 to represent no significant anomaly. A number of our LA-ICPMS analyses on a variety of different phases show a Ce anomaly

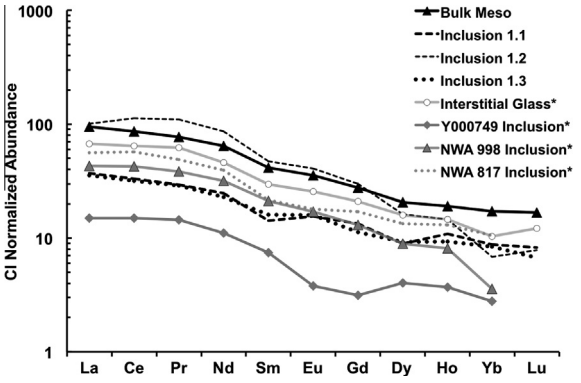

Fig. 13. Chondrite-normalized REEs in MIL 03346 mesostasis and olivine melt inclusion phases. *MIL 03346 intercumulus glass (Day et al., 2006); Y000749, NWA 998, and NWA 817 glassy olivine inclusions (Wadhwa et al., 2004) are also plotted.

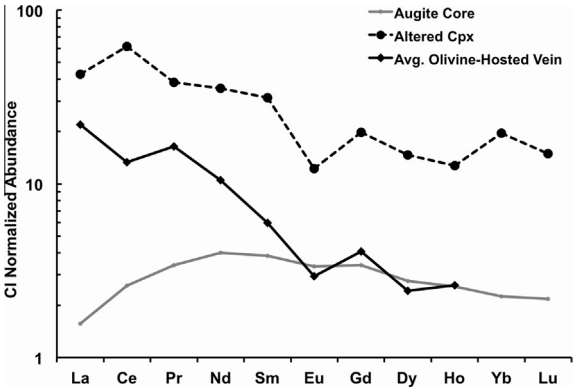

Fig. 14. Chondrite-normalized REEs in augite and related phases. Si-enriched olivine-hosted veins average REE abundances are also plotted for comparison.

(Table 4). However, no LREE enrichment or Ce anomaly was observed in the bulk mesostasis, olivine melt inclusions, and the interstitial Fe-rich olivine. Augite is also generally free of Ce anomalies. The olivine-hosted veins typically have small negative Ce anomalies except one point, which has a positive anomaly of 1.4. Fe,Ti-oxides in the mesostasis may have a slight negative Ce anomaly, and the altered augite has a small positive Ce anomaly.

4. DISCUSSION

The chemistry of secondary mineral phases is a function of: (1) the concentration of an element (or chemical component) in solution, which partly depends upon the source material and mobility; (2) the ability to be incorporated into the precipitate; and (3) the chemistry of the weathering environment, particularly pH and Eh of solution and the water/rock ratio. Si-enriched alteration products in nakhlites, including iddingsite and more poorly crystalline materials, mainly occur as veins in olivine and fill in void spaces. These veins are pre-terrestrial in Nakhla (Reid and Bunch, 1975; Gooding et al., 1991), Lafayette (Treiman et al., 1993) and Y000593 and Y000749 (Treiman and Goodrich, 2002)

Table 4
Ce anomalies[a] in MIL 03346.

	Altered olivine				Olivine melt inclusion						
	1	2			1	2	3				
Ce/Ce*	0.5	0.4			1.0	1.1	1.0				
	Olivine-hosted vein										
	1	2	3	4	5	6	7	8	9	10	11
Ce/Ce*	1.4	0.8	0.6	0.6	0.7	0.7	0.8	0.6	0.7	0.7	0.6
	Augite										Altered augite
	1	2	3	4	5	6	7	8	9		1
Ce/Ce*	1.1	0.8	1.0	1.0	0.8	0.9	1.0	1.0	1.2		1.5
	Bulk mesostasis				Meso fayalite		Meso Fe, Ti-oxide				
	1	2	3		1		1	2	3		
Ce/Ce*	1.0	1.0	1.0		1.0		0.9	–	0.7		

–, cannot be calculated because at least one element is below detection limits.
[a] Calculated using CI-normalized abundances.

where they are crosscut by the fusion crust and/or generally display degradation near this crust resulting from thermal devolatilization (e.g.,Velbel, 2012). A martian origin is inferred for the olivine-hosted veins in the other nakhlites based on their similar occurrence and chemistry. A martian origin is also inferred here for these veins in MIL 03346. One of these veins is truncated by a terrestrial weathering surface (Fig. 4), implying that it existed prior to the meteorite's residence in Antarctica. Other olivine-hosted alteration veins are vesiculated within a few hundred microns of the fusion crust (Fig. 9), consistent with thermal metamorphism and devolatilization of pre-terrestrial materials during the meteorite's passage through Earth's atmosphere.

Olivine-hosted alteration veins observed in MIL 03346 have elevated weight percentages of SiO_2, Al_2O_3, and SO_3 relative to unaltered olivine and are enriched in SiO_2 relative to the incipiently-altered areas (Table 2). Furthermore, the incipiently-altered olivine patches are enriched in Si and S compared to unaltered olivine. During aqueous processing (presumably on Mars), elements like Si and S may be incorporated in relatively small secondary phases (such as sulfates, very poorly crystalline phyllosilicates including montmorillonite, and/or silica) precipitated in the voids created by olivine dissolution. Al abundances differ within nakhlite alteration veins (Treiman et al., 1993; Gillet et al., 2002; Changela and Bridges, 2011; this study), implying local variations in solution chemistry and resulting secondary products as well as low fluid/rock ratios. The variable amounts of Fe, K, and S-enriched materials, differences in degree of crystallinity, and the range of morphologies associated with the olivine-hosted veins suggest variable degrees of weathering within and amongst nakhlites and could indicate, in some cases, interaction between pre-terrestrial Si-enriched veins and terrestrial solution.

Table 5 summarizes chemical differences in olivine-hosted alteration veins among the nakhlites. In MIL 03346, the olivine-hosted alteration veins are more Ca-poor than those in Lafayette or Nakhla and similar to those observed in NWA 817, which are smectite-bearing (Gillet et al., 2002). The FeO/SiO_2 and MgO/SiO_2 ratios of olivine and its alteration products in MIL 03346 trend toward smectite, similar to the trends observed by Gooding et al. (1991), Treiman et al. (1993), Kuebler et al. (2004), and Changela and Bridges (2011) for other nakhlites (Fig. 5). Given the Fe, Mg, Ca, and Al abundances of olivine and its alteration products in Miller Range nakhlites, Hallis and Taylor (2011) concluded that the olivine-hosted veins are likely a heterogeneous mixture of Fe-rich phyllosilicates and fine-grained Fe-oxides as had been previously proposed for iddingsite in other nakhlites. Some olivine-hosted veins in MIL 03346 shown in Fig. 5 are shifted towards the SiO_2-poor axis as a result of the presence of Fe($\pm$K)-sulfates (including jarosite) or Fe-oxides. MIL 03346 also has higher SO_3 abundances than Nakhla or Lafayette, but on the whole, the olivine alteration products in MIL 03346 are compositionally similar to smectite, though we did not observe well-formed phyllosilicates and, thus, true iddingsite as defined by Eggleton (1984) and Smith et al. (1987). The olivine-hosted veins are more consistent with the poorly crystalline, often amorphous, alteration products observed in other nakhlites (e.g., Changela and Bridges, 2011).

The negative Eu anomalies in MIL 03346 olivine-hosted veins and secondary phases associated with augite (Figs. 12 and 14) indicate that plagioclase has not contributed significant Eu to the solution, consistent with the slower dissolution rate of plagioclase compared to olivine at low pH (e.g., Chen and Brantley, 1997). For NWA 817 and Lafayette, Bridges and Grady (2000) and Gillet et al. (2002) cite the positive Eu anomalies measured in olivine-hosted alteration veins as evidence for significant plagioclase dissolution. Nakhla and Governador Valadares do not have Eu anomalies in the olivine-hosted alteration veins (Bridges and Grady, 1999, 2000).

Olivine melt inclusions 1.1 and 1.3 have REE patterns similar to the whole rock (Fig. 13), consistent with crystallization of the rock as a closed system. Inclusion 1.2 is greatly enriched in LREEs compared to the other two analyses of this melt inclusion. The high abundances of LREEs in NWA 998 were cited by Wadhwa et al. (2004) as probable evidence of terrestrial alteration in that meteorite, as these elements should be more soluable than the HREEs.

Table 5
Olivine "iddingsite" and similar phases (oxide wt.%).

	MIL 03346[a]	MIL 03346[b]	NWA 817[c]	NWA 998[d]	Y000593[e]	Y000749[f]	Lafayette[g]	Lafayette[h]	Nakhla[i]	Governador Valadares[j]
SiO_2	0.0	44.98	42.82	37.44	51.4	49.1	42.2	49.1	40.2	43.5
TiO_2	0.05	0.05	0.06	*	–	0.02	0.04	0.01	0.02	0.03
Al_2O_3	0.10	0.22	0.21	1.02	0.56	3.49	4.55	4.77	0.74	0.07
Cr_2O_3	*	0.06	0.03	*	–	–	0.02	*	0.03	*
FeO	0.0	36.65	36.45	39.66	25.66	28.80	27.2	29.01	31.4	31.2
MnO	0.62	0.65	0.55	0.61	0.22	0.15	0.48	0.48	0.63	0.52
MgO	3.11	3.10	5.69	4.14	3.80	7.49	9.9	13.9	6.82	8.23
CaO	0.13	0.07	0.25	3.04	0.08	0.45	1.18	0.70	1.14	0.20
Na_2O	*	*	0.18	0.05	–	0.13	0.22	0.30	*	0.37
K_2O	*	–	0.41	0.49	0.52	0.55	0.60	0.41	0.60	0.57
SO_3	1.02	*	–	–	2.79	–	–	0.69	0.14	0.16
Cl	–	–	–	–	–	–	–	0.36	0.66	0.74
SUM	5.03	85.77	86.65	86.44	85.03	90.18	86.39	99.73	82.38	85.59

–, not measured.
[a] This study, average of 5.
[b] Day et al. (2006), average of 4.
[c] Gillet et al. (2002), average of 25.
[d] Treiman and Irving (2008), average of 3.
[e] Noguchi et al. (2009).
[f] Treiman and Goodrich (2002).
[g] Kuebler et al. (2004), average of 29.
[h] Treiman et al. (1993), average of 83.
[i] Gooding et al. (1991), average of 78.
[j] Changela and Bridges (2011), average of 4.
* Below detection limits.

Therefore, the observed enrichment in REEs lighter than Ho in MIL 03346 melt inclusions might also be evidence of terrestrial aqueous alteration. Only inclusion 1.2 is enriched over bulk mesostasis for LREEs, making this the most likely candidate for any aqueous alteration. McCubbin et al. (2009) found a jarosite-bearing melt inclusion in a clinopyroxene grain, suggesting interaction with hydrothermal fluids in MIL 03346. However, the absence of a clear Ce anomaly in our analysis of olivine-melt inclusions, combined with little textural evidence of aqueous processing, suggests that the REE concentrations reflect primary melt compositions rather than alteration. Thus olivine-hosted melt inclusions do not appear to have significantly contributed to solution chemistry during aqueous alteration.

Phosphate may be enriched in olivine alteration veins, but olivine phenocrysts are probably not a significant contributor of phosphate to solution. It is also unlikely that augite could contribute enough phosphate to solution to account for the elevated abundances in crack-filling materials found in augite grains, considering the limited alteration of augite observed in MIL 03346. This suggests that the fluid was enriched in phosphorus from a different source, possibly interstitial phosphates or glass. Furthermore, the very low abundance of REEs in unaltered olivine suggests that the REE enrichment in the olivine-hosted alteration veins is inherited from components in solution other than those derived from the olivine.

The enrichment of REEs and other trace elements in the olivine-hosted alteration veins, incipiently-altered olivine, and altered augite (Figs. 12 and 14) may be attributed to the early dissolution of mesostasis phases such as REE-bearing chlorapatite and/or glass. The REEs in interstitial glass are somewhat less abundant than in the bulk mesostasis, which is a mixture of glass, phosphates, plagioclase, feldspar, Fe-rich olivine, sulfides, and Fe,Ti-oxides (Fig. 13). Chondrite-normalized REE abundances for titanomagnetite indicate that it is not a significant reservoir of REEs. However, REE abundances of interstitial glass from Day et al. (2006) show that these glasses in MIL 03346 are important reservoirs of REEs, and their dissolution may play a role in releasing REEs to solution in MIL 03346. The elevated abundances of Cs, Rb, and Ba in both the mesostasis and olivine alteration products combined with the low abundance in olivine (Fig. 11) suggest that these elements were also mobilized from the mesostasis, perhaps resulting from the dissolution of glassy phases during aqueous alteration in a closed system, and are deposited from solution in the olivine-hosted alteration veins.

The olivine-hosted alteration veins, incipiently-altered olivine, and altered augite are also enriched in Th and Pb. The bulk of the Th and Pb in MIL 03346 is concentrated in phases in the mesostasis. The relative enrichment of Th in olivine-hosted alteration products suggests that it is at least partially mobile. Depending on the conditions of alteration, certain elements may be mobile or immobile in solution (e.g., Price et al., 1991; Patino et al., 2003; Velbel et al., 2009). Th is not typically considered a mobile element in terrestrial weathering profiles; however, its apparent lack of mobility can result from adsorption and precipitation before it can be transported out of the system (e.g., Daux et al., 1994; Patino et al., 2003). If Th is somewhat mobile

in MIL 03346, it might suggest a proximal source, such as residual phases in the mesostasis such as phosphates. Th solubility can increase significantly in acidic conditions (e.g., Langmuir and Herman, 1980), and thus might occur on Mars if conditions are favorable.

Phosphates can dissolve somewhat faster than olivine at low pH (e.g., Wogelius and Walther, 1992; Guidry and Mackenzie, 2003), and because there is abundant evidence for the alteration of olivine, it is plausible that phosphates are affected as well. The martian origin of the olivine-hosted iddingsite-like veins suggests that the observed REE enrichment is, therefore, a product of pre-terrestrial alteration. Acid leaching experiments of Dreibus et al. (2008) on Zagami and a terrestrial basalt illustrate that REEs, with the exception of Eu, are readily mobilized during acidic leaching and can be widely distributed before re-precipitation. These leaching experiments illustrated that residual material has an overall REE-depletion, a stronger LREE-depletion, and a positive Eu anomaly, while the solution carries an enrichment of REEs, particularly LREEs, and a negative Eu-anomaly.

Two lines of evidence are often cited as indicators of terrestrial alteration: the formation of positive and/or negative Ce anomalies and LREE enrichments (e.g., Shimizu et al., 1983; Gooding, 1986; Floss and Crozaz, 1991; Mittlefehldt and Lindstrom, 1991; Crozaz and Wadhwa, 2001; Crozaz et al., 2003). Ce anomalies and/or LREE enrichments are often assumed to be the result of terrestrial weathering, in part based on their occurrence in meteorite finds rather than falls, and because pre-terrestrial Ce anomalies are generally not expected (e.g., Mittlefehldt and Lindstrom, 1991). A bulk analysis of the shergottite find Dhofar 019 revealed a pronounced positive Ce anomaly, while maskelynite exhibited an LREE depletion with a small negative Ce anomaly that were attributed to terrestrial weathering, consistent with the presence of abundant secondary calcite and sulfate in the meteorite and surrounding soils (Taylor et al., 2002). While Dreibus et al. (2008) do not favor a terrestrial origin for the strong LREE-depletions observed in martian meteorites found in Antarctica, some terrestrial redistribution of REEs is also possible. Ce anomalies can be created if Ce^{3+} is oxidized to Ce^{4+}, and the oxidized Ce is less mobile in solution.

Floss and Crozaz (1991) found that the patches of silica most affected by Antarctic alteration in the LEW85003 eucrite display REE enrichments and negative Eu anomalies similar to those we observe in MIL 03346. Mittlefehldt and Lindstrom (1991) measured positive Eu anomalies, loss of LREEs, and Ce anomalies that are particularly associated with the exteriors of Antarctic eucrites where terrestrial solutions would have the most access to mineral grains. Loss of LREEs, relative immobility of Eu, and variable Ce mobility in Antarctic eucrites might result from a redistribution of elements from meteorite exteriors to internal precipitates (i.e., incorporation of LREEs, negative Eu anomalies, and variable Ce anomalies) during aqueous alteration. Therefore, similar LREE enrichments, negative Eu anomalies, and variable Ce anomalies in MIL 03346 could result from either interactions with terrestrial solutions or in comparable martian conditions.

The olivine-hosted alteration veins in MIL 03346 are enriched in all detectable REEs, including HREEs (Fig. 12), and REE enrichments in the Si-enriched olivine-hosted veins are generally correlated to negative Ce anomalies. In NWA 817, the olivine-hosted veins have a distinct V-shaped REE pattern that Gillet et al. (2002) attribute to martian weathering processes rather than a terrestrial LREE-enrichment, partly owing to the lack of a Ce anomaly. Olivine-hosted alteration veins in the other nakhlites (including Nakhla) do not have Ce anomalies (Bridges and Grady, 1999, 2000; Gillet et al., 2002), so it is possible that at least some of the REE pattern and Ce anomalies in MIL 03346 are attributed to terrestrial alteration. However, the absence of Ce anomalies does not necessarily imply an absence of terrestrial weathering; amorphous alteration veins in shergottites Dar al Gani 476 and Dar al Gani 489 show enriched LREEs but no Ce anomaly (Crozaz and Wadhwa, 2001; Crozaz et al., 2003).

Similar REE enrichments and corresponding negative Ce anomalies are reported in, for example, some terrestrial basalt weathering profiles (Ludden and Thompson, 1979; Price et al., 1991; Patino et al., 2003) and, as discussed above, for eucrite LEW85300 (Floss and Crozaz, 1991). Patino et al. (2003) attributed the enrichment of REEs and relative depletion of Ce^{4+} in the terrestrial basalts to a local pH increase in part of the weathering profile. Floss and Crozaz (1991) suggested the source of the REEs in the eucrite are dissolved Ca-phosphates. A terrestrial alteration component to REE distribution and/or redistribution in MIL 03346 seems likely and is consistent with the survey of Crozaz et al. (2003) who found that the highest levels of terrestrial REE movement in meteorites from both hot and cold deserts occurred along cracks and defects in a meteorite, resulting in a concentration of REEs in vein-filling materials.

It is not clear at this time the extent to which the measured Ce anomalies in MIL 03346 (Table 4) result from terrestrial alteration. The obvious Antarctic weathering effects on and near the surface of the meteorite shows that the meteorite has been exposed long enough for chemical changes to occur, but the question yet remains as to how far into the meteorite this alteration may extend. It is possible that much of the observed alteration is terrestrial in origin, and separating terrestrial from martian alteration may be difficult.

Preliminary H-isotopic studies of individual secondary phases in martian meteorites produced mixed results. Vicenzi et al. (2007b) measured D/H ratios of jarosite in the interior of MIL 03346 and found the isotopic composition to be consistent with a non-terrestrial origin. Recent analysis by Hallis et al. (2011) on Nakhla and MIL 03346 found significant terrestrial water contamination on the surfaces of the Si-enriched olivine-hosted alteration veins. Heating the samples removed some of this water, but still resulted in a D/H ratio within the error of the expected terrestrial value. Similar analyses on sulfates in shergottites Roberts Massif 04262 (Greenwood et al., 2009) and QUE 94201 (Ross et al., 2010) have also produced D/H ratios consistent with contamination from terrestrial water. The isotopic composition of jarosite in both shergottites is con-

sistent with an Antarctic origin, but the authors could not rule out a martian origin combined with a recent re-equilibration under terrestrial conditions. Therefore, at this time, it is not yet clear from H-isotopes alone how much, if any, of the alteration products in MIL 03346 are martian in origin. What is clear, however, is that, if they were formed on Mars, significant isotopic changes have taken place during contact with the terrestrial environment.

The problem is similar in the case of Ce oxidation, as terrestrial alteration may re-work the chemical signatures of martian minerals. It may be possible for similar alteration processes on Mars and the Earth to result in similar chemical signatures, such as Ce anomalies, under favorable conditions, that cannot be easily differentiated from each other. Oxidation is expected to be slow on Mars in acidic solutions (Burns, 1993); however, in low water/rock ratios, pH, and solution chemistry can change, and perhaps Ce is oxidized. Martian jarosite identified by the Mars Exploration Rover Opportunity at Meridiani Planum (e.g., Klingelhofer et al., 2004) requires at least partial oxidation of Fe^{2+} to Fe^{3+} for its formation. Thus, it seems likely that martian water is oxidizing enough to create Ce anomalies. Chennaoui Aoudjehane et al. (2012) report LREE enrichments and small positive Ce anomalies in the shergottite Tissint (a recent fall in Morocco), which they attribute to the incorporation of oxidized Mars surface soils or leachates prior to shock melting. Therefore, the variability in Ce anomalies among analyses within MIL 03346 may reflect local changes in solution chemistry typical of water-limited regimes on Mars. However, if the Ce anomalies in MIL 03346 are pre-terrestrial, then similar Ce anomalies are expected in all of the nakhlite meteorites (especially the only fall, Nakhla), which is not the case.

Finally, MIL 03346 olivine alteration products are more enriched in SO_3 than other nakhlites except for Y000593 and Y000749 (Fig. 5D). A trend of increasing SO_3 with increasing alteration is common for many martian rocks and soils (recent review in King and McLennan, 2010), suggesting that the sulfur signature of MIL 03346 may have been acquired while on Mars. However, the presence of Ca-sulfates in what appear to be post-impact cracks throughout MIL 03346 sections implies that the Ca-sulfates may have been emplaced at a later time and from a different solution than the olivine-hosted veins, perhaps a second aqueous event that was enriched in Ca, S, and REEs, and a possible terrestrial origin cannot be ruled out. In fact, a terrestrial origin is the most likely explanation as sulfur is found enriched near the Antarctic weathering surfaces of MIL 03346 (Figs. 4 and 10B). In the sections examined in this study, Ca-sulfates were not observed to crosscut the olivine alteration veins; however, they do crosscut the fusion crust (Fig. 10A). Velbel (2012) reported Ca-sulfates partially filling vesicles in the fusion crust of MIL 03346. These observations indicate at least some of the Ca-sulfates are terrestrial precipitates. Ca-sulfate is also commonly found in cracks or voids in pyroxenes or the mesostasis, and other S-bearing phases are present in the olivine-hosted veins and cracks.

5. CONCLUSIONS

The composition and occurrence of Si-enriched, olivine-hosted alteration veins in MIL 03346 are consistent with their formation on Mars. The variable composition (i.e., Al) of these veins suggests a water-limited alteration regime where microenvironments control the formation of secondary products from solution. The range of vein morphologies from simple to complex forms suggests variable aqueous conditions over time. The distribution and abundance of elements in these alteration products are consistent with the mobilization of elements from susceptible mineral phases, such as phosphates and residual glass, during aqueous processes. Under favorable conditions, these phases can dissolve more readily than pyroxenes, plagioclase, and even olivine at low pH. The low abundances of Na and K as well as the lack of positive Eu anomalies in the olivine-hosted veins are consistent with a virtually no plagioclase dissolution from the mesostasis. Such limited plagioclase dissolution may be common on Mars (e.g., Hurowitz and McLennan, 2007). Degree of alteration in MIL 03346 is variable and is generally greater near surfaces exposed to the elements in Antarctica as well as along fractures. The concentration of sulfates near the edge of the meteorite (Hallis and Taylor, 2011), in fusion crust vesicles (Velbel, 2012), in post-impact cracks and voids, and crosscutting the fusion crust (Vicenzi et al., 2007b; Velbel, 2012; this study) suggests a terrestrial origin for these precipitates. Local heterogeneities in MIL 03346 alteration products and chemical signatures suggest variability in solution chemistry over mm-scales, consistent with small pore spaces and limited availability of water that could occur on Mars. However, enrichments in REEs in olivine alteration products generally also correlate with negative Ce anomalies potentially owing to terrestrial alteration. Thus, elevated S and REE abundances in MIL 03346 alteration products may indicate a strong enrichment of these elements in a martian fluid, or, more likely, these chemical signatures result from terrestrial overprinting during the meteorite's residence in Antarctica.

ACKNOWLEDGEMENTS

This research was primarily funded by a Grant from the NASA Graduate Student Researcher Program (J.D. Stopar, Awardee). Additional support was provided by NASA Mars Fundamental Research Program grant NNG05GL77G (M.A. Velbel, P.I.) and the NASA Astrobiology Institute under Cooperative Agreement No. NNA09DA77A (J.G. Taylor). Helpful reviews were provided by Bradley L. Jolliff (Washington University in St. Louis, MO, USA) and an anonymous reviewer.

REFERENCES

Barrat J. A., Benoit M. and Cotten J. (2006) Bulk chemistry of the nakhlite Miller Range 03346 (MIL 03346). *Lunar Planet. Sci. Conf. XXXVII*. #1569 (abstr.).

Berkeley J. L., Keil K. and Prinz M. (1980) Comparative petrology and origin of Governador Valadares and other nakhlites. *Proc. Lunar Planet. Sci. Conf.* **11**, 1089–1102.

Bridges J. C. and Grady M. M. (1999) A halite–siderite–anhydrite–chlorapatite assemblage in Nakhla: mineralogical evidence for evaporites on Mars. *Meteorit. Planet. Sci.* **34**, 407–415.

Bridges J. C. and Grady M. M. (2000) Evaporite mineral assemblages in the nakhlite (martian) meteorites. *Earth Planet. Sci. Lett.* **176**, 267–279.

Bridges J. C., Catling D. C., Saxton J. M., Swindle T. D., Lyon I. C. and Grady M. M. (2001) Alteration assemblages in martian meteorites: implications for near-surface processes. *Space Sci. Rev.* **96**, 365–392.

Bunch T. E. and Reid A. M. (1975) The nakhlites, Part I: petrography and mineral chemistry. *Meteoritics* **10**, 303–315.

Burns R. G. (1993) Rates and mechanisms of chemical weathering of ferromagnesian silicate minerals on Mars. *Geochim. Cosmochim. Acta* **57**, 4555–4574.

Changela H. G. and Bridges J. C. (2011) Alteration assemblages in the nakhlites: variation with depth on Mars. *Meteorit. Planet. Sci.* **45**, 1847–1867.

Chen Y. and Brantley S. L. (1997) Temperature- and pH-dependence of albite dissolution rates at acid pH. *Chem. Geol.* **135**, 275–290.

Chennaoui Aoudjehane H., Barrat J.-A., Boudouma O., Chen G., Duke M. J. M., Franchi I. A., Gattacceca J., Grady M. M., Greenwood R. C., Herd C. D. K., Hewins R., Jambon A., Marty B., Rochette P., Smith C. L., Sautter V., Verchovsky A., Weber P. and Zanda B. (2012) Tissint martian meteorite: a fresh look at the interior, surface, and atmosphere of Mars. *Science* **338**, 785–788.

Crozaz G. and Wadhwa M. (2001) The terrestrial alteration of Saharan shergottites Dar al Gani 471 and 489: a case study of weathering in a hot desert environment. *Geochim. Cosmochim. Acta* **65**, 971–978.

Crozaz G., Floss C. and Wadhwa M. (2003) Chemical alteration and REE mobilization in meteorites from hot and cold desert. *Geochim. Cosmochim. Acta* **67**, 4727–4741.

Daux V., Crovisier J. L., Hemond C. and Petit J. C. (1994) Geochemical evolution of basaltic rocks subjected to weathering: fate of the major elements, rare earth elements, and thorium. *Geochim. Cosmochim. Acta* **58**, 4941–4954.

Day J. M. D., Taylor L. A., Floss C. and McSween, Jr., H. Y. (2006) Petrology and chemistry of MIL 03346 and its significance in understanding the petrogenesis of nakhlites on Mars. *Meteorit. Planet. Sci.* **41**, 581–606.

Dreibus G., Haubold R., Huisl W. and Spettel B. (2008) The loss of K, REE, Th, and U from a martian and a terrestrial basalt by acidic leaching. *Meteorit. Planet. Sci.* **43**, 1895–1908.

Dyar M. D., Treiman A. H., Pieters C. M., Hiroi T., Lane M. D. and O'Conner V. (2005) MIL 03346, the most oxidized Martian meteorite: a first look at spectroscopy, petrography, and mineral chemistry. *J. Geophys. Res.* **110**, E09005. http://dx.doi.org/10.1029/2005JE002426.

Eggleton R. A. (1984) Formation of iddingsite rims on olivine: a transmission electron microscope study. *Clays Clay Mineral.* **32**, 1–11.

Floss C. and Crozaz G. (1991) Ce anomalies in the LEW85300 eucrite: evidence for REE mobilization during Antarctic weathering. *Earth Planet. Sci. Lett.* **107**, 13–24.

Freidman Lentz R. C., Taylor G. J. and Treiman A. H. (1999) Formation of a martian pyroxenite: a comparative study of the nakhlite meteorites and Theo's flow. *Meteorit. Planet. Sci.* **34**, 919–932.

Fries M., Rost D., Vicenzi E. and Steele A. (2006) Raman imaging analysis of jarosite in MIL 03346. Workshop on martian sulfates as recorders of atmospheric–fluid–rock interactions, October 22–24, 2006 in Houston, Texas. LPI Contribution No. 1331, abstract 7060.

Gillet P., Barrat J. A., Deloule E., Wadhwa M., Jambon A., Sautter V., Devouard B., Neuville D., Benzerara K. and Lesourd M. (2002) Aqueous alteration in the Northwest Africa 817 (NWA 817) martian meteorite. *Earth Planet. Sci. Lett.* **203**, 431–444.

Gooding J. L. (1978) Chemical weathering on Mars. *Icarus* **33**, 483–513.

Gooding J. L. (1986) Weathering of stony meteorites in Antarctica. International Workshop on Antarctic Meteorites, pp. 48–54.

Gooding J. L., Wentworth S. J. and Zolensky M. E. (1991) Aqueous alteration of the Nakhla meteorite. *Meteoritics* **26**, 135–143.

Greenwood J. P., Itoh S., Sakamoto N. and Yurimoto H. (2009) Hydrogen isotope measurements of gypsum and jarosite in martian meteorite Roberts Massif 04262: Antarctic and Houstonian weathering. *Lunar Planet. Sci. Conf. XL*. #2528 (abstr.).

Guidry M. W. and Mackenzie F. T. (2003) Experimental study of igneous and sedimentary apatite dissolution: control of pH, distance from equilibrium, and temperature on dissolution rates. *Geochim. Cosmochim. Acta* **67**, 2949–2963.

Hallis L. J. and Taylor G. J. (2011) Comparisons of the four Miller Range nakhlites, MIL 03346, 090030, 090032 and 090136: textural and compositional observations of primary and secondary mineral assemblages. *Meteorit. Planet Sci.* **46**, 1787–1803.

Hallis L. J., Taylor G. J., Stopar J. D., Velbel M. A. and Vicenzi E. P. (2011) Martian vs. terrestrial alteration assemblages in MIL 03346 and Nakhla: hydrogen isotope and compositional comparisons. *Lunar Planet. Sci. Conf*. 42. #1442 (abstr.).

Hicks T. L. (2002) Automated mapping and modal analysis of meteorite thin sections using image processing software. MS Thesis, University of Hawaii.

Hurowitz J. A. and McLennan S. M. (2007) A ~3.5 Ga record of water-limited, acidic weathering conditions on Mars. *Earth Planet. Sci. Lett.* **260**, 432–443.

Imae N. and Ikeda Y. (2007) Petrology of the Miller Range 03346 nakhlite in comparison with the Yamato-000593 nakhlite. *Meteorit. Planet. Sci.* **42**, 171–184.

Imae N., Ikeda Y., Shinoda K., Kojima H. and Iwata N. (2003) Yamato nakhlites: petrography and mineralogy. *Antarct. Meteor. Res.* **16**, 13–33.

King P. L. and McLennan S. M. (2010) Sulfur on Mars. *Elements* **6**, 107–112.

Klingelhofer G., Morris R. V., Bernhardt B., Schroder C., Rodionov D. S., de Souza, Jr., P. A., Yen A., Gellert R., Evlanov E. N., Zubkov B., Foh J., Bonnes U., Kankeleit E., Gutlich P., Ming D. W., Renz F., Wdowiak T., Squyres S. W. and Arvidson R. E. (2004) Jarosite and hematite at Meridiani Planum from Opportunity's Mossbauer spectrometer. *Science* **306**, 1740–1745.

Kuebler K., Jolliff B. L., Wang A. and Haskin L. A. (2004) A survey of olivine alteration products using Raman spectroscopy. *Lunar Planet. Sci. Conf. XXXV*. #1704 (abstr.).

Kuebler K., Jolliff B. L. and Treiman A. (2007) A survey of alteration products and other secondary minerals in martian meteorites recovered from Antarctica. *Lunar Planet. Sci. Conf. XXXVIII*. #2228 (abstr.).

Langmuir D. and Herman J. S. (1980) The mobility of thorium in natural waters at low temperatures. *Geochim. Cosmochim. Acta* **44**, 1753–1766.

Loughnan F. C. (1969) *Chemical Weathering of the Silicate Minerals*. American Elsevier Publishing Company, New York, 154 p.

Ludden J. N. and Thompson G. (1979) An evaluation of the behavior of the rare earth elements during the weathering of sea–floor basalt. *Earth Planet. Sci. Lett.* **43**, 85–92.

McCubbin F. M., Tosca N. J., Smirnov A., Nekvasil H., Steele A., Fries M. and Lindsley D. H. (2009) Hydrothermal jarosite and hematite in a pyroxene-hosted melt inclusion in martian meteorite Miller Range (MIL) 03346: implications for magmatic-hydrothermal fluids on Mars. *Geochim. Cosmochim. Acta* **73**, 4907–4917.

Mittlefehldt D. W. and Lindstrom M. M. (1991) Generation of abnormal trace element abundances in Antarctic eucrites by weathering processes. *Geochim. Cosmochim. Acta* **55**, 77–87.

Noguchi T., Nakamura T., Misawa K., Imae N., Aoki T. and Toh S. (2009) Laihunite and jarosite in the Yamato 00 nakhlites: alteration products on Mars? *J. Geophys. Res.* **114**, E10004. http://dx.doi.org/10.1029/2009JE003364, 2009.

Norman M. D., Pearson N. J., Sharma A. and Griffin W. L. (1996) Quantitative analysis of trace elements in geological materials by laser ablation ICPMS: instrumental operating conditions and calibration values of NIST glasses. *Geostand. Newslett.* **20**, 247–261.

Norman M. D., Garcia M. O. and Bennett V. C. (2004) Rhenium and chalcophile elements in basaltic glasses from Ko'olau and Moloka'i volcanoes: magmatic outgassing and composition of the Hawaiian plume. *Geochim. Cosmochim. Acta* **68**, 3761–3777.

Palme H. and Beer H. (1993) Abundances of the elements in the solar system. In Landolt-Börnstein, Group VI: Astronomy and Astrophysics: Instruments; Methods; Solar System (ed. H. H. Voigt). Springer, Berlin, vol. 3(a), pp. 196–221.

Palme H. and Jones A. (2003) Solar system abundances of the elements. In *Treatise on Geochemistry* (eds. H. D. Holland and K. K. Turekian), Elsevier, vol. 1, pp. 41–61.

Patino L. C., Velbel M. A., Price J. R. and Wade J. A. (2003) Trace element mobility during spheroidal weathering of basalts and andesites in Hawaii and Guatamala. *Chem. Geol.* **202**, 343–364.

Price R. C., Gray C. M., Wilson R. E., Frey F. A. and Taylor S. R. (1991) The effects of weathering on rare-earth element, Y and Ba abundances in Tertiary basalts from southeastern Australia. *Chem. Geol.* **93**, 245–265.

Reid A. M. and Bunch T. E. (1975) The nakhlites – II: where, when, and how. *Meteoritics* **10**, 317–324.

Righter K. and McBride K. M. (2011) The Miller Range nakhlites: a summary of the curatorial subdivision of the main mass in light of newly found paired masses. *Lunar Planet. Sci. Conf. 42*. #2161 (abstr.).

Robertson K. and Bish D. (2007) The dehydration kinetics of gypsum: the effect of relative humidity on its stability and implications in the martian environment. *Lunar Planet. Sci. Conf. XXXVIII*. #1432 (abstr.).

Ross D. K., Ito M., Rao M. N., Hervig R., Williams L. B., Nyquist L. E. and Peslier A. (2010) Jarosite in the shergottite QUE 94201. *Lunar Planet. Sci. Conf*. 41. #1154 (abstr.).

Sautter V., Barratt J. A., Jambon A., Lorand J. P., Gillet Ph., Javoy M., Joron J. L. and Lesourd M. (2002) A new martian meteorite from Morocco: the nakhlite North West Africa 817. *Earth Planet. Sci. Lett.* **195**, 223–238.

Shimizu H., Masuda A. and Tanaka T. (1983) Cerium anomaly in REE pattern of Antarctic eucrite. *Mem. Natl. Inst. Polar Res. Spec. Issue* **30**, 341–348.

Smith K. L., Milnes A. R. and Eggleton R. A. (1987) Weathering of basalt: formation of iddingsite. *Clays Clay Mineral.* **35**, 418–428.

Swindle T. D. and Olson E. K. (2004) ^{40}Ar–^{39}Ar studies of whole rock nakhlites: evidence for the timing of formation and aqueous alteration on Mars. *Meteorit. Planet. Sci.* **39**, 755–766.

Taylor G. J., Stopar J. D., Boynton W. V., Karunatillake S., Keller J. M., Bruckner J., Wanke H., Dreibus G., Kerry K. E., Reedy R. C., Evans L. G., Starr R. D., Martel L. M. V., Squyres S. W., Gasnault O., Maurice S., dUston C., Englert P., Dohm J. M., Baker V. R., Hamara D., Janes D., Sprague A. L., Kim K. J., Drake D. M., McLennan S. M. and Hahn B. C. (2006) Variations in K/Th on Mars. *J. Geophys. Res.* **111**, E03S06. http://dx.doi.org/10.1029/2006JE002676 (printed 112(E3), 2007).

Taylor L. A., Nazarov M. A., Shearer C. K., McSween, Jr., H. Y., Cahill J., Neal C. R., Ivanova M. A., Barsukova L. D., Lentz R. C., Clayton R. N. and Mayeda T. K. (2002) Martian meteorite Dhofar 019: a new shergottite. *Meteorit. Planet. Sci.* **37**, 1107–1128.

Treiman A. H. (2005) The nakhlite meteorites: augite-rich igneous rocks from Mars. *Chem. Erde* **65**, 203–270.

Treiman A. H. and Goodrich C. A. (2002) Pre-terrestrial aqueous alteration of the Y-000593 and Y-000749 nakhlite meteorites. *Proc. NIPR Symp. Antarct. Meteorit.* **27**, 166–167.

Treiman A. H. and Irving A. J. (2008) Petrology of martian meteorite Northwest Africa 998. *Meteorit. Planet Sci.* **43**, 829–854.

Treiman A. H. and Lindstrom D. J. (1997) Trace element geochemistry of martian iddingsite in the Lafayette meteorite. *J. Geophys. Res.* **102**(E4), 9153–9163.

Treiman A. H., Barrett R. A. and Gooding J. L. (1993) Preterrestrial aqueous alteration of the Lafayette (SNC) meteorite. *Meteoritics* **28**, 86–97.

Udry A., McSween, Jr., H. Y., Lecumberri-Sanchez P. and Bodnar R. J. (2012) Paired nakhlites MIL 090030, 090032, 090136, and 03346: insights into the Miller Range parent meteorite. *Meteorit. Planet. Sci.* **47**, 1575–1589.

Velbel M. A. (2009) Dissolution of olivine during natural weathering. *Geochim. Cosmochim. Acta* **73**, 6098–6113.

Velbel M. A. (2012) Aqueous alteration in martian meteorites: comparing mineral relations in igneous-rock weathering of martian meteorites and in the sedimentary cycle of Mars. *Sediment. Geol. Mars SEPM Spec. Publ.* **11**, 97–117.

Velbel M. A., Donatelle A. R. and Formolo M. J. (2009) Reactant–product textures, volume relations, and implications for major-element mobility during natural weathering of hornblende, Tallulah Falls Formation, Georgia Blue Ridge, U.S.A. *Am. J. Sci.* **309**, 661–688.

Velbel M. A., Stopar J. D., Taylor G. J. and Vicenzi E. P. (2010) Aqueous alteration of olivine in Mars meteorite MIL03346: corrosion textures and redistribution of elements in alteration products. *Lunar Planet. Sci. Conf. 41*. #2223 (abstr.).

Vicenzi E. P., Fries M., Fahey A., Rost D., Greenwood J. P. and Steele A. (2007a) Detailed elemental, mineralogical, and isotopic examination of jarosite in martian meteorite MIL 03346. *Lunar Planet. Sci. Conf. XXXVIII*. #2335 (abstr.).

Vicenzi E. P., Fries M., Fahey A., Rost D., Greenwood J. P. and Steele A. (2007b) Evidence for young jarosite precipitation on Mars. 70th Annual Meteoritical Society Meeting, August 13–17, 2007, Tucson, Arizona. *Meteorit. Planet. Sci. Suppl. 42*. #5293 (abstr.).

Wadhwa M. and Crozaz G. (1995) Trace and minor elements in minerals of nakhlites and Chassigny: clues to their petrogenesis. *Geochim. Cosmochim. Acta* **59**, 3629–3645.

Wadhwa M. and Crozaz G. (2003) Trace element geochemistry of new nakhlites from the Antarctic and Saharan desert: further constraints on nakhlite petrogenesis on Mars. *Lunar Planet. Sci. XXXIV*. #2075 (abstr.).

Wadhwa M., Crozaz G. and Barrat J.-A. (2004) Trace element distributions in the Yamato 000593/000749, NWA 817 and NWA 998 nakhlites: implications for their petrogenesis and mantle sources on Mars. *Antarct. Meteorit. Res.* **17**, 97–116.

Wentworth S. J., Gibson E. K., Velbel M. A. and McKay D. S. (2005) Antarctic Dry Valleys and indigenous weathering in Mars meteorites: implications for water and life on Mars. *Icarus* **174**, 383–395.

Wogelius R. A. and Walther J. V. (1992) Olivine dissolution kinetics at near-surface conditions. *Chem. Geol.* **97**, 101–112.

Associate editor: Christian Koeberl